Zootaxa 4532 (2): 203–230
http://www.mapress.com/j/zt/

Article

ISSN 1175-5326 (print edition)
ZOOTAXA
ISSN 1175-5334 (online edition)

https://doi.org/10.11646/zootaxa.4532.2.2
http://zoobank.org/urn:lsid:zoobank.org:pub:18EFD994-C314-4E9A-A658-CC2BBE32C6EA

A new species of *Phyzelaphryne* Heyer, 1977 (Anura: Eleutherodactylidae) from the Japurá River basin, with a discussion of the diversity and distribution of the genus

PEDRO IVO SIMÕES[1,7], JOÃO CARLOS LOPES COSTA[2], FERNANDO J. M. ROJAS-RUNJAIC[1, 3], GIUSSEPE GAGLIARDI-URRUTIA[1], MARCELO JOSÉ STURARO[2,4], PEDRO L. V. PELOSO[2,5] & SANTIAGO CASTROVIEJO-FISHER[1,6]

[1] *Laboratório de Sistemática de Vertebrados / Programa de Pós-Graduação em Zoologia, Escola de Ciências, Pontifícia Universidade Católica do Rio Grande do Sul, Av. Ipiranga 6681, Prédio 40, sala 110, 90619-900, Porto Alegre, Rio Grande do Sul, Brazil.*
[2] *Laboratório de Herpetologia, Museu Paraense Emílio Goeldi / CZO, CP 399, Av. Perimetral, 1901, Terra Firme, 66077-530 Belém, Pará, Brazil.*
[3] *Fundación La Salle de Ciencias Naturales, Museo de Historia Natural La Salle, Apartado Postal 1930, Caracas 1010–A, Venezuela.*
[4] *Universidade Federal de São Paulo, Departamento de Ecologia e Biologia Evolutiva, Av. Professor Artur Riedel, 275, Jardim Eldorado, Diadema, CEP 09972-270, São Paulo, Brazil.*
[5] *Universidade Federal do Pará, Instituto de Ciências Biológicas, R. Augusto Corrêa, 1, Guamá, Belém, 66075-110, Pará, Brazil.*
[6] *Department of Herpetology, American Museum of Natural History, Central Park West & 79th St., New York, NY 10024, USA.*
[7] *Corresponding author. E-mail: pedroivosimoes.bio@gmail.com*

Abstract

We describe and name the second species of *Phyzelaphryne* (Brachycephaloidea, Eleutherodactylidae), from northwestern Brazilian Amazonia. *Phyzelaphryne nimio* **sp. nov.** is distinguished from its only congener, *Phyzelaphryne miriamae*, by its smaller body size and the anatomy of the carpal and metacarpal regions, with relatively larger (sometimes fused) supernumerary carpal and metacarpal tubercles. Molecular phylogenetic analyses based on fragments of the mitochondrial genes 16S rRNA and COI suggest that the currently known distribution of the species is restricted to its type locality and other areas within Estação Ecológica Juami-Japurá, state of Amazonas, Brazil. Based on molecular, morphological and bioacoustic evidence, we assigned other specimens recently collected in Parque Nacional do Jaú, state of Amazonas, Brazil, to *P. miriamae*, extending the species' known geographic distribution north of the Amazon River.

Key words: Amazonia, Brazil, conservation units, DNA barcoding, morphology, Phyzelaphryninae, Terrarana

Resumo

Descrevemos e nomeamos a segunda espécie de *Phyzelaphryne* (Brachycephaloidea, Eleutherodactylidae), a partir de espécimes coletados no noroeste da Amazônia brasileira. *Phyzelaphryne nimio* **sp. nov.** se distingue da única outra espécie do gênero, *Phyzelaphryne miriamae*, por seu tamanho corporal menor e pela anatomia das regiões carpal e metacarpal, com tubérculos carpais e metacarpais supra-numerários relativamente maiores (algumas vezes fusionados). Análises filogenéticas moleculares baseadas em fragmentos dos genes mitocondriais 16S rRNA e COI indicaram que a distribuição da nova espécie é restrita à sua localidade tipo e a outras áreas da Estação Ecológica Juami-Japurá, no Estado do Amazonas, Brasil. Com base em evidências moleculares, morfológicas e bioacústicas, nós designamos outros espécimes coletados recentemente no Parque Nacional do Jaú, Amazonas, Brasil, como *P. miriamae*, ampliando a distribuição geográfica conhecida da espécie ao norte do rio Amazonas.

Palavras-chave: Amazônia, Brasil, unidades de conservação, DNA barcoding, morfologia, Phyzelaphryninae, Terrarana

Accepted by M. Rivera-Correa: 31 Oct. 2018; published: 18 Dec. 2018

Introduction

Phyzelaphryne Heyer, 1977 is a monotypic genus of direct-developing froglets that are locally abundant, but hardly detectable inhabitants of the leaf litter in Amazonia (Fouquet *et al.* 2012; Frost 2018). Advances in the taxonomy of the genus have been partially hampered by the paucity of collected specimens, which can be largely attributed to their small body size, cryptic dorsal colors and overall morphological similarity among evolutionary lineages uncovered by molecular phylogenetic approaches (Hoogmoed & Lescure 1984; Fouquet *et al.* 2012).

Since the original description and definition, the systematics of the genus—for which the only named species is *Phyzelaphryne miriamae* Heyer, 1977—has been reasonably stable. After Lynch (1980) synonymized *P. miriamae* with *Hypodactylus nigrovittatus* (Andersson, 1945), based largely on the inspection of published data, Hoogmoed & Lescure (1984) conducted a thorough morphological analysis of the type series of *P. miriamae* and similar specimens. Hoogmoed & Lescure's (1984) analysis resulted in the resurrection of *Phylezaphryne*, the description of a new genus (*Adelophryne* Hoogmoed & Lescure, 1984), and the description of diagnostic characters for both taxa. In summary, *Adelophryne* and *Phyzelaphryne* are characterized by the presence of laterally grooved, pointed discs on fingers and toes, by a single subarticular tubercle or hump on finger IV and by a narrow head, with eyes projecting outwards, beyond head circumference in dorsal view. *Adelophryne* and *Phyzelaphryne* can be distinguished from each other by the morphology of some elements of hands and feet. *Adelophryne* has reduction of phalanges, flattening of digits and presence of flattened or indistinct palmar and plantar tubercles (defined as "pads" by some authors, but see Material and Methods below), while *Phyzelaphryne* present individualized and well-developed tubercles (Hoogmoed & Lescure 1984; MacCulloch *et al*. 2008).

Recent phylogenetic studies based on mitochondrial and nuclear DNA sequences recovered *Adelophryne* and *Phyzelaphryne* as sister taxa (Hedges *et al.* 2008; Fouquet *et al.* 2012; Padial *et al.* 2014; Heinicke *et al.* 2018). Furthermore, Fouquet *et al.* (2012) also reported high levels of genetic diversity among samples of *Phyzelaphryne* collected across Amazonia, suggesting that several unnamed species exist in the genus. Also, according to Fouquet *et al.* (2012), *Phyzelaphryne* has a primarily southern Amazonian geographic distribution, south of the Solimões/Amazon River (Hedges *et al.* 2008; Fouquet *et al.* 2012), with a single locality (Leticia, Colombia) north of the river.

Two recent expeditions to sites north of the Solimões/Amazon River (Japurá and Negro River basins) resulted in the collection of a large series of additional specimens of *Phyzelaphryne.* We used this new material to perform an integrative analysis of molecular, morphological and bioacoustic characters. Our analyses revealed that these specimens include representatives of the two major clades of *Phyzelaphryne* reported by Fouquet *et al.* (2012). The specimens from the Japurá River drainage represent a new species that we describe herein, whereas those from Rio Negro are *P. miriamae* and constitute the first record of that species north of the Amazon River.

Material and methods

Institutional abbreviations and acronyms used throughout the text are: MCP (Museu de Ciências e Tecnologia, Pontifícia Universidade Católica do Rio Grande do Sul, Brazil); MPEG (Coleção Herpetológica Osvaldo Rodrigues da Cunha, Museu Paraense Emilio Goeldi, Belém, Brazil); MZUSP (Museu de Zoologia da Universidade de São Paulo, São Paulo, Brazil); USNM (Smithsonian Institution, National Museum of Natural History, Washington D.C., USA).

Recent Collections. Specimens studied here were collected in two field expeditions to two different areas in the state of Amazonas, Brazil (Fig. 1). The first expedition was conducted in Parque Nacional do Jaú (PNJ hereafter). This national park comprises 9,194 km^2 of mostly pristine tropical rainforest, including seasonally flooded and *terra-firme* rainforests, as well as small patches of open vegetation, such as *campinas* and *campinaranas*, roughly characterized by the dominance of short trees with thin stems, growing on white-sand soils. Several sampling points were established along both banks of the Jaú River, where we used pitfall traps, acoustic and visual surveys. *Phyzelaphryne* specimens were collected at a single *terra-firme* locality (2.29417° S, 62.45583 W; 53–55 m a.s.l.) between 25–27 February 2017.

The second expedition was to Estação Ecológica Juami-Japurá (EEJJ hereafter), located on the south bank of the middle Japurá River. This conservation unit comprises 8,315 km^2 of Amazon forest habitat, including both seasonally flooded and *terra-firme* rainforests. *Phyzelaphryne* specimens were collected between 02–09 February

2017 at two *terra-firme* forest sampling sites: (i) Canal da Inveja, with trails established in a *terra-firme* forest landscape on the west bank of the Juami River along its lower course (1.75834° S, 67.61532° W; 62–67 m a.s.l); and (ii) Igarapé da Fartura, with trails through *terra-firme* forests on the east bank of the middle course of the Juami River (1.96063° S, 67.93694° W; 71–87 m a.s.l.).

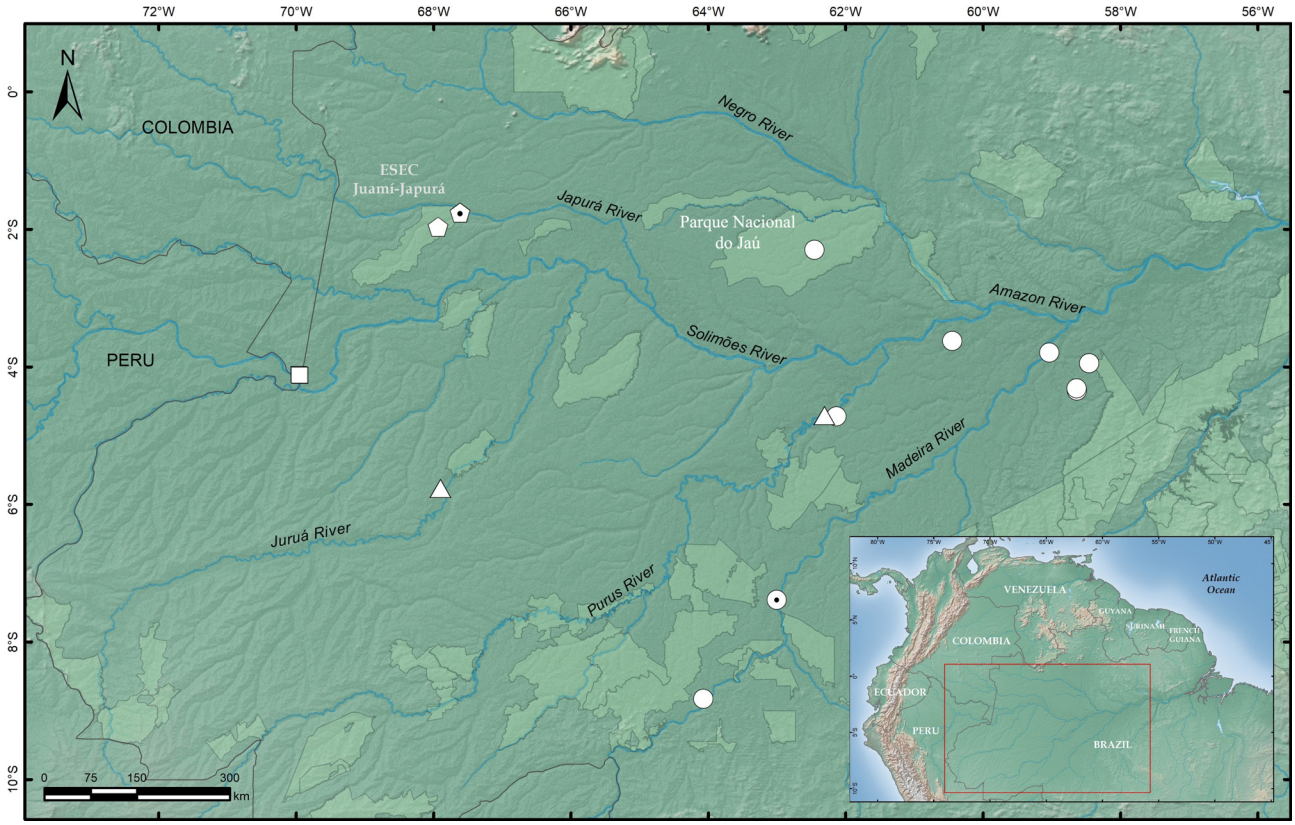

FIGURE 1. Geographic location of study areas in Brazilian Amazonia (Estação Ecológica Juami-Japurá and Parque Nacional do Jaú) and known localities of *Phyzelaphryne* based in Hoogmoed & Lescure (1984), Fouquet *et al.* (2012) and the results of this study. Lighter green shades correspond to Brazilian conservation units and black dots mark type localities. Pentagons, *P. nimio* **sp. nov.**; circles, *P. miriamae*; Triangles and square, *Phyzelaphryne* sp. (C1) and *Phyzelaphryne* sp. (C2), respectively, two candidate new species.

Specimens found among the forest leaf litter in both study areas were captured manually and transported to improvised laboratories in the field. All specimens were anesthetized and killed with topical benzocaine solution (50 mg/g), fixed in 10 % formalin solution and preserved in 70 % ethanol. A sample of muscular tissue was dissected from a hind limb of each specimen prior to fixation and preserved in 95–100 % ethanol for molecular studies. Specimens from PNJ are housed in the amphibian collection at MPEG (MPEG 41041–41045), whereas specimens from EEJJ are housed in the amphibian collection of MCP (MCP 13683–13725).

Phylogenetic analyses. We used DNA sequences of two mitochondrial genes—the Ribosomal Subunit 16S rRNA (16S) and Cytochrome Oxidase 1 (COI)—commonly used on amphibian barcoding and phylogenetics, including Phyzelaphryninae (Fouquet *et al*. 2012; Padial *et al*. 2014), to investigate the phylogenetic relationships of the newly collected material with regards to previously published sequences.

New sequences were generated for eight specimens from three localities: four from EEJJ (MCP 13687, 13710, 13711, 13719), three from PNJ (MPEG 41041, 41044, 41045), and a specimen from Floresta Nacional de Pau-Rosa available at MPEG (MPEG 28548). Total genomic DNA was extracted from preserved tissue samples using either DNEasy (Qiagen) or Wizard Genomic (Promega, Madison-WI, USA) DNA purification kits following manufacturer instructions. Polymerase chain reactions (PCR) were performed in 25.0 µL volumes with 2.0 µL of genomic DNA. For the 16S fragment (~ 566 bp) we used the universal primers 16Sar (5′-CGCCTGTTTATCAAAAACAT-3′) and 16Sbr (5′-CCGGTCTGAACTCAGATCACGT-3′) (Palumbi 1996), whereas for the COI fragment (~ 658 bp) we used the primers COI.PF-A (5-TTTCAACHAAYCAYAAAGAYATYGG-3’) and COI.PR-A (5’-TANACTTCNGGGTGDCCAAARAATCA-3’)

(Peloso *et al.* 2014). PCR and DNA sequencing protocols followed those in Peloso *et al.* (2014; 2016). Resulting sequences were manually edited using the original chromatograms in Sequencher 4.1.4 (Gene Codes Corporation, Ann Arbor, MI, USA) or Geneious 9.1.8 (Kearse *et al.* 2012).

We downloaded from GenBank (Benson *et al.* 2013) all available homologous sequences of specimens of *Phyzelaphryne*. Additionally, we included sequences of representatives of Amazonian *Adelophryne* species. Abbreviations (C1 or C2) were used to indicate new candidate species not yet described (see Discussion and Figure 2). We used sequences of *Eleutherodactylus limbatus* to root all trees. Detailed information on samples used is in Appendix 1.

Sequences were aligned using MAFFT v7.309 (Katoh *et al*. 2013). We used the alignment strategy Q-INS-i for 16S and Auto for COI, both with default parameters. Concatenation of genes was performed using the program Sequence Matrix v1.7.8 (Vaidya *et al*. 2011). The best scheme for data partitions—with a maximum of four partitions corresponding to 16S and the three codon positions of COI—was selected using the software PartitionFinder 2 (Lanfear *et al*. 2016), using the Bayesian Information Criterion (BIC) and the "greedy" search algorithm (Lanfear *et al*. 2012) with "linked" branch lengths.

Maximum Likelihood analyses were carried out in the CIPRES Science Gateway (Miller *et al*. 2010) using Garli 2.01 (Zwickl 2006) implementing the partitions and models selected by PartitionFinder and considering indels as unknown nucleotides. We ran 500 independent tree searches, in order to avoid the use of sub-optimal trees, and 1000 non-parametrical bootstrap (BS) pseudoreplicates (Felsenstein 1985).

Parsimony tree searches were performed in TNT (Goloboff *et al*. 2008; equal costs for all transformations, non-additive characters, and indels treated as fifth state) using the new technologies option at level 50 and finding the minimum length 100 times. We calculated jackknife (JK) frequencies from 1000 pseudoreplicates searched with 100 RAS + TBR and a maximum of 100 trees saved per replicate, gaps treated as fifth state, and removal probability of 0.36 (~ e-1), which purportedly renders jackknife and bootstrap values comparable (Farris *et al*. 1996).

To assess genetic distances among samples of Amazonian Phyzelaphryninae, we calculated uncorrected-pairwise and Kimura-2-parameter genetic distances using a similarity alignment of the longest possible fragment (*i.e.*, no missing data) of the gene 16 rDNA, which includes the most frequently used barcode in amphibians (Vences *et al.* 2005). Distances were estimated in MEGA 7.1 (Kumar *et al.* 2015).

Advertisement calls. We obtained advertisement calls of males of *Phyzelaphryne* from two localities. From PNJ we used recordings from two males, obtained by PLVP on 27 February 2017. Recordings were made using a Marantz PMD 620 digital recorder with internal microphone positioned approximately 0.5 m from the focal male. The recordings were made between 17:48–18:10h at a sampling rate of 44.1 kHz and 16-bit resolution. Air temperature was not recorded. Both specimens were collected and deposited into the MPEG collection (MPEG 41044, 41045).

The other recording was of a male *Phyzelaphryne miriamae* recorded by PIS near Cachoeira do Teotônio, on the left bank of the Madeira River, in Rondônia, Brazil (8.828611° S, 64.074722° W; 97 m a.s.l.), ~ 190 km southwest of the type locality of *P. miriamae* at Igarapé Puruzinho, on the same riverbank. The recording was made at 18:26h, on 05 November 2010, at an air temperature of 25.6 °C, using a Marantz PMD 660 digital recorder and a Sennheiser ME 66/K6 directional microphone positioned approximately 0.5 m from the focal male. The recording was conducted at a sampling rate of 44.1 kHz and 16-bit resolution. The calling male was not collected, but was photographed while being recorded, which allows for a confident identification of the species. Unfortunately, no calling males were found at EEJJ and we have no available calls from that population.

From each recording, we selected 10 calls uniformly distributed along its length. The number of pulses per note, call duration, duration of notes and duration of silent intervals between notes and calls were measured from oscillograms. Peak (*i.e.*, dominant frequency), upper and lower frequencies of notes and of the whole call were measured from power spectrum graphs. Spectral analyses were conducted with frequency resolution of 164 Hz and 2048 points, using Blackman window type. Upper and lower frequencies of notes were measured 20 dB below peak frequency intensity, in order to avoid overlap with background noise. Values of acoustic parameters of notes and call are presented as the averages among the mean values of recorded focal males. Bioacoustic terminology followed Köhler *et al.* (2017). All acoustic analyses were conducted in Raven Pro 1.4 (Bioacoustics Research Program 2011).

Morphology. Adult specimens were sexed using primary and secondary sexual characters: presence of vocal slits in males, presence of mature oocytes visible through skin in females. Preserved specimens were examined and measured to the nearest 0.1 mm under a stereomicroscope with graduated lenses. Morphometric measurements and diagnostic characters followed Heyer (1977) and Hoogmoed & Lescure (1994), with the addition of measurements

documented in descriptions of other small anuran taxa commonly found among the forest leaf litter (Lourenço-de-Moraes *et al*. 2014; Simões 2016). For the specific case of palmar and plantar external morphology, we followed Kok & Kalamandeen (2008) and Duellman & Lehr (2009). Flattened, horizontally expanded or indistinct supernumerary and subarticular tubercles on ventral surfaces of hands and feet were termed "pads" or "subdigital pads" in taxonomic studies of *Adelophryne* (*e.g*., Hoogmoed & Lescure 1994; Lourenço-de-Moraes *et al*. 2014). We refrained from using this terminology because the word "pad" is frequently applied to refer to the skin on the underside of the discs on tips of fingers and toes in other Terrarana (Duellman & Lehr 2009), and described the morphology of supernumerary and subarticular tubercles instead.

Measurements were taken as follows: Snout-vent length (SVL); head length from tip of snout to posterior edge of maxilla articulation (HL); head width at the level of maxilla articulation (HW); snout length from anterior corner of the eye to tip of snout (SL); eye-to-nostril distance from anterior corner of the eye to the center of nostril (EN); internarial distance between internal edge of of nostrils (IN); eye length from anterior to posterior corner (EL); interorbital distance, measured at the level of the narrowest distance between orbits (IO); horizontal diameter of tympanum (TYM); forearm length from proximal edge of the largest palmar tubercle to outer edge of flexed elbow (FAL); upper arm length from anterior corner of arm insertion on body to the outer edge of flexed elbow (UAL); lengths of fingers from proximal edge of palmar tubercle to tips of fingers I, II, III, and IV (respectively HAND I, HAND II, HAND III, HAND IV); width of disc on Finger III (WFD); width of Finger III's distal phalange, at its middle level (WPF); maximum diameter of the largest palmar tubercle (DPT); maximum diameter of thenar tubercle (DTET); leg length from the posterior extremity of the coccyx to the outer edge of flexed knee (LL); tibia length from outer edge of flexed knee to heel (TL); tarsus length from the outer edge of flexed knee to the proximal edge of outer metatarsal tubercle (TAL); foot length from proximal edge of outer metatarsal tubercle to tip of Toe IV (FL); width of disc on Toe IV (WTD); width of distal phalanx of Toe IV at its midpoint (WTP); maximum diameter of outer metatarsal tubercle (DoTAT); maximum diameter of inner metatarsal tubercle (DiTAT).

A preserved female specimen from EEJJ (MCP 13720) was cleared and stained for examination of skeletal traits of fingers and toes. After removal of skin, gonads, digestive tract and lungs, the specimen was immersed in 100 mL absolute ethanol for 24 hours, transferred to 100 mL solution of 70 mL absolute ethanol, 30 mL acetic acid and 0.1 g alcian blue for 24 hours, digested in 100 mL of 0.1 g trypsin solution for 24 hours, and stained in 100 mL of 1.5 % KOH solution and 0.1 g alizarin red for 24 hours. The specimen was then immersed in 100 mL glycerin / 1.5 % KOH solution with increasing glycerin concentration every 24 hours (40 %, 70 %, 95 %) and permanently stored in 95 % glycerin.

For comparison, we examined and photographed the holotype (MZUSP 49894, a female) and some of the paratypes (MZUSP 49895, USNM 239363, USNM 202607, 202608) of *Phyzelaphryne miriamae*. We also examined several specimens in the MPEG collection, which are assigned to *P. miriamae*: MPEG 5205, MPEG 5275 (Brazil, Amazonas, Coari, Porto Urucu); MPEG 5581, MPEG 5622 (Brazil, Amazonas, Benjamin Constant); MPEG 14019–14022 (Brazil, Amazonas, Careiro da Várzea, Estrada para Autazes); MPEG 28548–28549 (Brazil, Amazonas, Maués, Floresta Nacional de Pau-Rosa).

Results

Phylogenetic analyses. The aligned dataset includes 1,586 sites, *i.e.*, transformation series (928 bp of 16S and 658 bp of COI). Parsimony analysis found six equally parsimonious trees (length = 2,217 transformations). The strict consensus (not shown) is identical to the best tree from the ML analysis (Fig. 2) except for three polytomies involving intraspecific relationships. The best partition scheme and corresponding models were: 16S (GTR+G), COI first position (TrN+G), COI second position (TrNef+I+G) and COI third position (HKY+I). The optimal ML tree (ln = -9995.417499; Fig. 2) recovered *Adelophryne* and *Phyzelaphryne* as reciprocally monophyletic. *Phyzelaphyne miriamae* is monophyletic (BS and JK = 100) and shows a marked phylogeographic structure, with uncorrected genetic distances = 0–5 % (Table 1). Specimens from PNJ fall within *P. miriamae*. Specimens from EEJJ are also monophyletic (BS and JK = 100) and more closely related to the candidate new species *Phyzelaphryne* sp. (C1) and *Phyzelaphryne* sp. (C2) reported by Fouquet *et al.* (2012) than to *P. miriamae*. Genetic distances are summarized in Table 1.

Morphological comparisons. Several external morphological character states were shared between specimens from PNJ and specimens in the type series of *Phyzelaphryne miriamae*, as well as other referred specimens (Table

2, Fig. 3): dorsum uniformly brown, with pale brown blotches present only on dorsal surfaces of limbs and snout of some specimens (Fig. 3); venter light brown with tiny cream spots, uniformly scattered on throat, chest and abdomen; three round to elliptical supernumerary tubercles are present on fingers in all specimens; a supernumerary tubercle is present at the base of finger IV; supernumerary tubercles are protuberant, separated by conspicuous gaps in all specimens. SVL of male specimens from PNJ ranged from 15.5 to 16.2 mm, slightly larger than male specimens in the type series of *P. miriamae* (14.6–15.1 mm). Head width was also larger among specimens from PNJ (5.6–5.9 mm) than male paratypes of *P. miriamae* (4.8–50 mm). Other measurements overlapped in range between species in the *P. miriamae* type series and specimens collected in PNJ.

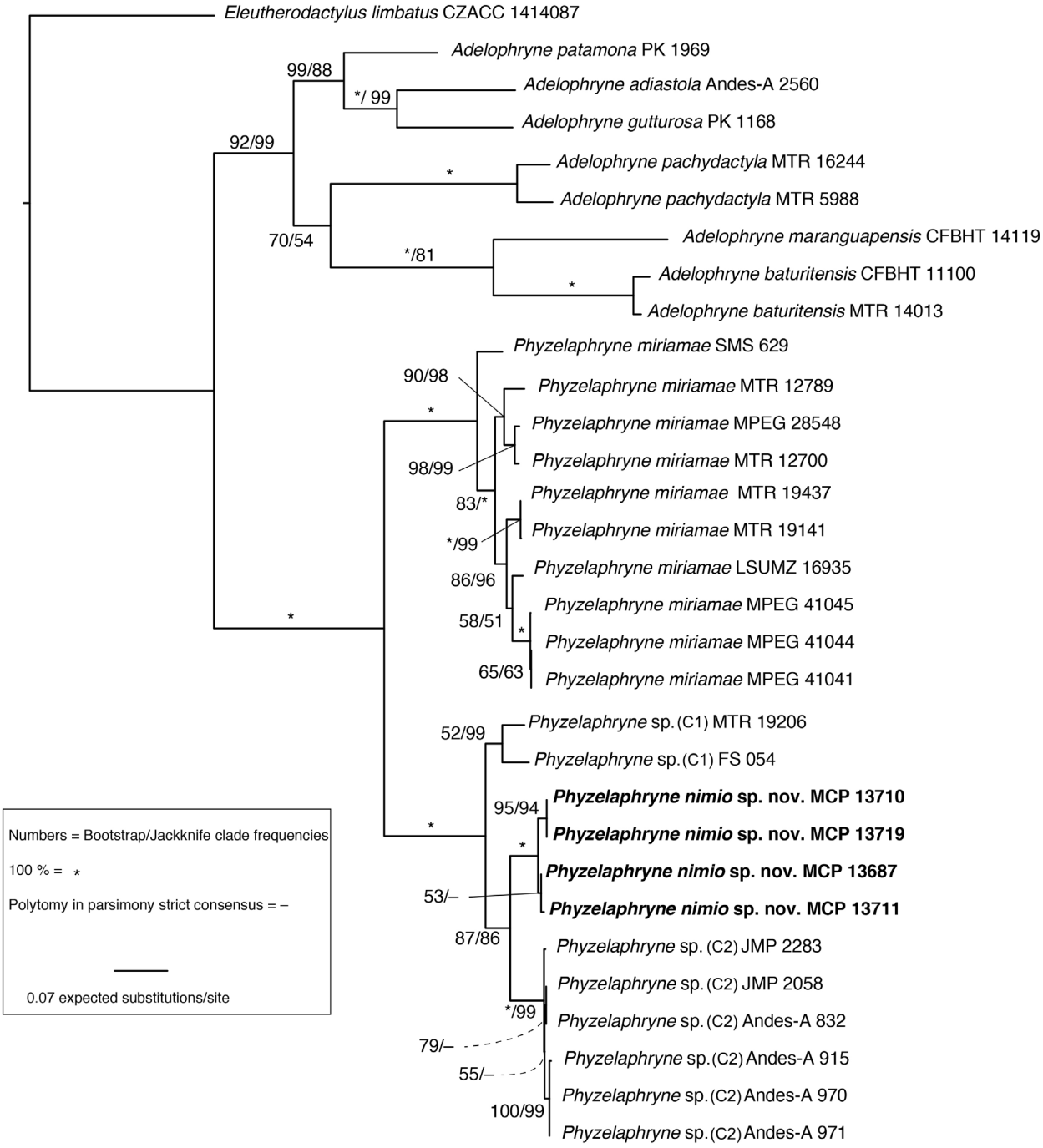

FIGURE 2. Phylogenetic hypothesis inferred from a maximum likelihood analysis (ln = -9995.417499) of concatenated DNA sequences of genes 16S and COI (1,586 pb) of Phyzelaphryninae. *Eleutherodactylus limbatus* is used as outgroup.

TABLE 1. Percentage of uncorrected pairwise and Kimura-2-parameter genetic distances (below and above the diagonal, respectively) between *Phyzelaphryne nimio* **sp. nov.** and other Amazonian Phyzelaphryninae. Distances were based in a 404 bp fragment of the mitochondrial 16S rDNA. General locality of each sample in parentheses but see detailed information in Appendix 1.

	1	**2**	**3**	**4**	**5**	**6**	**7**	**8**	**9**	**10**	**11**	**12**	**13**	**14**	**15**	**16**	**17**	**18**	**19**	**20**	**21**	**22**	**23**	**24**
1. P. nimio MCP 13719 (EEJJ)		0	1	1	15	14	14	14	14	14	13	15	15	15	5	5	4	4	4	4	4	26	21	26
2. *P. nimio* MCP 13710 (EEJJ)	0		1	1	15	14	14	14	14	14	13	15	15	15	5	5	4	4	4	4	4	26	21	26
3. *P. nimio* MCP 13711 (EEJJ)	1	1		0	14	15	14	14	14	15	14	15	15	15	4	4	4	4	4	4	4	26	22	25
4. *P. nimio* MCP 13687 (EEJJ)	1	1	0		15	15	14	14	14	15	14	16	16	15	4	5	4	4	4	4	4	25	22	25
5. *P. miriamae* SMS 629 (Purus)	12	12	12	12		5	3	4	4	4	3	5	5	5	12	14	14	14	14	14	14	24	22	23
6. *P. miriamae* MTR 12789 (Abacaxis)	12	12	12	12	4		3	4	4	4	3	6	6	6	13	16	15	15	15	15	16	24	20	24
7. *P. miriamae* MTR 12700 (Abacaxis)	11	11	12	12	3	2		4	4	3	0	5	5	5	13	15	15	15	15	15	15	25	21	24
8. *P. miriamae* MTR 19141 (Purus)	11	11	12	12	3	4	3		0	2	4	4	4	4	12	14	15	15	15	15	15	22	20	23
9. *P. miriamae* MTR 19437 (Purus)	11	11	12	12	3	4	3	0		2	4	4	4	4	12	14	15	15	15	15	15	22	20	23
10. *P. miriamae* LSUMZ 16935 (Manaquiri)	12	12	12	12	3	4	3	2	2		4	3	3	2	12	14	14	14	14	14	14	23	20	22
11. *P. miriamae* MPEG 28548 (Paraconi)	11	11	11	12	3	3	0	4	4	3		5	5	5	13	15	15	15	15	15	15	25	21	25
12. *P. miriamae* MPEG 41041 (PNJ)	12	12	12	13	4	5	5	4	4	2	5		0	0	13	14	14	14	14	14	14	24	23	23
13. *P. miriamae* MPEG 41044 (PNJ)	12	12	12	13	4	5	5	4	4	2	5	0		0	13	14	14	14	14	14	14	24	23	23
14. *P. miriamae* MPEG 41045 (PNJ)	12	12	12	12	4	5	4	3	3	2	5	0	0		12	13	14	14	14	14	14	24	22	23
15. *Phyzelaphryne* sp. (C1) MTR 19206 (Purus)	5	5	4	4	10	11	11	10	10	10	11	11	11	10		5	5	5	5	5	5	24	23	24
16. *Phyzelaphryne* sp.. (C2) Andes-A 915 (Leticia)	4	4	4	4	11	13	12	12	12	11	12	11	11	11	4		0	0	0	0	0	26	23	24
17. *Phyzelaphryne* sp. (C2) Andes- A 970 (Leticia)	4	4	4	4	12	12	12	12	12	12	12	11	11	11	4	0		0	0	0	0	25	22	24
18. *Phyzelaphryne* sp. (C2) Andes-A 971 (Leticia)	4	4	4	4	12	12	12	12	12	12	12	11	11	11	4	0	0		0	0	0	25	22	24
19. *Phyzelaphryne* sp. (C2) Andes-A JMP 2283 (Leticia)	4	4	4	4	12	12	12	12	12	12	12	11	11	11	4	0	0	0		0	0	25	22	24
20 *Phyzelaphryne* sp. (C2) Andes-A 832 (Leticia)	4	4	4	4	12	12	12	12	12	12	12	11	11	11	4	0	0	0	0		0	25	22	24
21. *Phyzelaphryne* sp.. (C2) Andes-A JMP 2058 (Leticia)	4	4	4	4	12	12	12	12	12	12	12	11	11	11	4	0	0	0	0	0		25	23	24
22. *A. adiastola* Andes-A 2560	19	19	19	19	17	18	18	17	17	17	18	18	18	18	18	19	18	18	18	18	19		12	13
23. *A. gutturosa* PK 1168	16	16	17	17	17	16	16	15	15	16	16	17	17	17	17	17	17	17	17	17	17	10		14
24. *A. patamona* PK 1969	19	19	19	19	17	17	17	17	17	16	18	17	17	17	18	18	18	18	18	18	18	11	12	

TABLE 2. Morphometric measurements (see Material and methods) and proportions of the holotypes of *Phyzelaphryne miriamae* and *P. nimio* **sp. nov.**, and summary of these variables (average ± one standard deviation, when sample size > 3, followed by range) of the paratypes of both species, separated by sex, and of the specimens collected at Parque Nacional do Jaú (PNJ).

	P. nimio			***P. miriamae***			
	Holotype	**Paratypes**		**Holotype**	**Paratypes**		**PNJ**
Variable	**Female**	**Females (n = 17)**	**Males (n = 18)**	**Female**	**Females (n=3)**	**Males (n = 2)**	**Males (n = 5)**
SVL	15.3	14.4 ± 0.8 (13.2–15.9)	12.1 ± 1.0 (11.2–15.2)	20.0	19.4–20.0	14.6–15.1	16 ± 0.3 (15.5–16.2)
HL	5.1	4.8 ± 0.3 (4.5–5.5)	4.3 ± 0.3 (3.9–4.9)	7.3	7.0–7.3	5.5–5.8	5.4 ± 0.2 (5.2–5.7)
HW	5.9	5.4 ± 0.2 (4.9–5.9)	4.6 ± 0.3 (4.1–5.2)	6.4	6.0–6.4	4.8–5.0	5.7 ± 0.1 (5.6–5.9)
SL	2.9	2.5 ± 0.3 (2.0–3.0)	2.2 ± 0.2 (1.8–2.6)	3.1	2.5–3.1	2.3–2.7	2.1 ± 0.1 (2.0–2.3)
EN	1.7	1.5 ± 0.1 (1.3–1.9)	1.3 ± 0.2 (0.8–1.7)	1.6			1.5 ± 0.1 (1.4–1.6)
IN	2.0	1.9 ± 0.1 (1.7–2.1)	1.6 ± 0.2 (1.0–1.9)	2.4			2.0 ± 0.1 (1.9–2.1)
EL	2.3	2.2 ± 0.1 (2–2.5)	2.0 ± 0.1 (1.8–2.2)	2.6–2.7*	2.3–2.7	2.2–2.4	2.2 ± 0.2 (2.1–2.5)
IO	2.1	1.7 ± 0.2 (1.5–2.1)	1.5 ± 0.1 (1.1–1.6)	2.1	2.1	1.8	3.4 ± 0.7 (3.1–3.6)
TYM	0.7	0.8 ± 0.1 (0.6–1)	0.7 ± 0.1 (0.6–0.8)	1.1–1.2	1.0–1.2	0.8	1.0 ± 0.0 (1.0–1.0)
FAL	3.9	3.6 ± 0.2 (3.3–4)	3.1 ± 0.2 (2.8–3.5)	4.5			4.2 ± 0.2 (4.1–4.5)
UAL	3.0	3.3 ± 0.3 (2.9–3.9)	2.7 ± 0.3 (2.4–3.5)	4.1			3.1 ± 0.1 (2.9–3.2)
HANDI	2.1	2.0 ± 0.1 (1.8–2.3)	1.6 ± 0.1 (1.4–1.9)	2.6			2.1 ± 0.1 (1.9–2.2)
HAND II	2.1	2.1 ± 0.1 (1.9–2.4)	1.7 ± 0.2 (1.4–2.1)	2.4			2.3 ± 0.1 (2.2–2.4)
HAND III	3.0	2.9 ± 0.2 (2.2–3.2)	2.4 ± 0.2 (2.1–2.9)	3.6			3.2 ± 0.1 (3.1–3.4)
HAND IV	2.0	1.9 ± 0.1 (1.7–2.0)	1.6 ± 0.2 (1.1–2.0)	2.5			2.1 ± 0.1 (2.0–2.2)
WFD	0.5	0.3 ± 0.1 (0.3–0.5)	0.3 ± 0.03 (0.2–0.4)	0.4			0.4 ± 0.0 (0.3–0.4)
WPF	0.3	0.3 ± 0.02 (0.3–0.4)	0.4 ± 0.4 (0.2–2.0)	0.3			0.3 ± 0.1 (0.3–0.4)
DPT	0.8	0.6 ± 0.1 (0.5–0.8)	0.6 ± 0.1 (0.5–0.8)	0.8			0.8 ± 0.1 (0.7–0.8)
DTET	0.5	0.5 ± 0.1 (0.4–0.7)	0.5 ± 0.1 (0.3–0.6)	0.6			0.7 ± 0.1 (0.6–0.8)
LL	7.5	7.2 ± 0.4 (6.5–7.9)	6.2 ± 0.4 (5.3–7.0)	9.2			7.8 ± 0.2 (7.6–8.0)

……continued on the next page

TABLE 2. (Continued)

	P. nimio			*P. miriamae*			
	Holotype	**Paratypes**		**Holotype**	**Paratypes**		**PNJ**
Variable	**Female**	**Females (n = 17)**	**Males (n = 18)**	**Female**	**Females (n=3)**	**Males (n = 2)**	**Males (n = 5)**
TL	7.5	7.3 ± 0.3 (6.7–7.9)	6.3 ± 0.4 (5.7–7.3)	8.8–8.9	7.5–8.9		7.5 ± 0.2 (7.2–7.7)
TAL	4.8	4.3 ± 0.3 (3.6–4.9)	3.7 ± 0.3 (3.2–4.5)	4.6			4.8 ± 0.3 (4.5–5.1)
FL	7.1	6.7 ± 0.4 (6.1–7.4)	5.9 ± 0.3 (5.3–6.8)	7.8			6.6 ± 0.1 (6.5–6.7)
WTD	0.6	0.6 ± 0.1 (0.5–0.7)	0.5 ± 0.05 (0.4–0.6)	0.6			0.5 ± 0.1 (0.4–0.6)
WTP	0.3	0.3 ± 0.05 (0.3–0.4)	0.3 ± 0.02 (0.3–0.4)	0.4			0.3 ± 0.1 (0.3–0.4)
DoTAT	0.4	0.4 ± 0.1 (0.3–0.5)	0.4 ± 0.05 (0.3–0.5)	0.4			0.4 ± 0.1 (0.3–0.4)
DiTAT	0.9	0.8 ± 0.1 (0.6–1.0)	0.6 ± 0.1 (0.5–0.9)	1.0			0.9 ± 0.1 (0.8–1.0)
HL/SVL	0.33	0.33 ± 0.02 (0.31–0.37)	0.35 ± 0.02 (0.31–0.40)	0.36			0.34 ± 0.01 (0.32–0.35)
HW/SVL	0.39	0.37 ± 0.02 (0.32–0.42)	0.38 ± 0.02 (0.34–0.41)	0.32			0.36 ± 0.01 (0.35–0.37)
HL/HW	0.86	0.90 ± 0.04 (0.83–0.96)	0.92 ± 0.03 (0.87–0.98)	1.1			0.95 ± 0.03 (0.89–0.97)
TYM/SVL	0.05	0.05 ± 0.01 (0.04–0.07)	0.06 ± 0.02 (0.05–0.07)	0.06			0.06 ± 0.00 (0.06–0.06)
FAL/SVL	0.25	0.25 ± 0.02 (0.22–0.30)	0.26 ± 0.02 (0.23–0.29)	0.22			0.27 ± 0.01 (0.26–0.28)
TL/SVL	0.49	0.51 ± 0.02 (0.47–0.55)	0.52 ± 0.03 (0.48–0.58)	0.44			0.47 ± 0.02 (0.45–0.50)

* Indicates original values of measurements by Heyer (1977) that were measured on both sides of the specimen.

TABLE 3. Structural, spectral and temporal properties (in Hz and s, respectively) of advertisement calls of two males of *Phyzelaphryne miriamae* (MPEG 41044, 41045) recorded in Parque Nacional do Jaú (PNJ), Amazonas, Brazil. These are compared to acoustic properties of calls of a male *P. miriamae* recorded at Cachoeira do Teotônio (CdT), on the left bank of the Madeira River, approximately 190 km southwest of the species type locality. Values are presented as mean ± one standard deviation (range), except for number of pulses on 1st and 2nd notes, presented as mode (range).

	PNJ (MPEG 41044)	**PNJ (MPEG 41045)**	**CdT**
# calls analyzed	10	10	10
Pulses on 1st note	3 (3–4)	3 (3–4)	2 (2–3)
Pulses on 2nd note	3 (2–3)	3 (2–3)	2 (2–3)
1st note lower frequency	2829.9 ± 69.6 (2756.2–2959.9)	2986.8 ± 73.5 (2851.4–3062.7	2952.5 ± 117.3 (2688.4–3109.3)
1st note upper frequency	4575.6 ± 184.0 (4331.2–4847.2)	4312.7 ± 79.7 (4157.1–4426)	4582.3 ± 212.5 (4262.8–4935.5)
1st note peak frequency	3811.3 ± 209.1 (3531.4–4069.8)	3837.2 ± 40.3 (3789.8–3897.5)	3617.6 ± 49.7 (3531.4–3703.7)
1st note duration	0.021 ± 0.001 (0.019–0.023)	0.016 ± 0.001 (0.014–0.019)	0.011 ± 0.003 (0.010–0.019)
Silent interval between notes	0.020 ± 0.002 (0.014–0.019)	0.020 ± 0.002 (0.017–0.022)	0.020 ± 0.001 (0.017–0.022)
2nd note lower frequency	2812.5 ± 82.0 (2729.1–2973.5)	2952.2 ± 55.5 (2889.8–3091.5)	2920.1 ± 148.7 (2742.7–3102.5)
2nd note upper frequency	4740.5 ± 322.2 (4331.2–5105.2)	4489.4 ± 130.5 (4320.4–4742.8)	4664.7 ± 215.2(4344.8–4983.0)
2nd note peak frequency	4005.2 ± 66.9 (3919–4091.3)	3843.7 ± 61.9 (3746.8–3940.6)	3819.9 ± 213.9 (3531.4–4091.3)
2nd note duration (s)	0.019 ± 0.003 (0.015–0.022)	0.0143 ± 0.001 (0.012–0.016)	0.012 ± 0.001 (0.01–0.014)
Call lower frequency (Hz)	2868.7 ± 96.2 (2701.9–2987.1)	2954.9 ± 56.4 (2870.6–3062.7)	2927.6 ± 78.6 (2810.6–3082.1)
Call upper frequency (Hz)	4657.1 ± 236.9 (4399.1–5078)	4429.2 ± 72.5 (4301.2–4512.4)	4741.4 ± 199.4 (4467–5002)
Call peak frequency	3968.2 ± 80.3 (3854.4–4069.8)	3852.3 ± 52.2 (3789.8–3940.6)	3764.0 ± 202.2 (3531.4–4048.2)
Call duration	0.057 ± 0.001 (0.055–0.059)	0.050 ± 0.001 (0.048–0.052)	0.043 ± 0.002 (0.041–0.047)
Silent interval between calls	3.954 ± 1.270 (2.052–5.670)	4.627 ± 1.793 (2.94–8.946)	5.486 ± 1.171 (4.313–8.203)

Specimens from EEJJ differed from specimens collected in PNJ and Coari, and from specimens in the type series of *Phyzelaphryne miriamae* in a set of morphological characters, such as morphology of palmar and plantar surfaces, morphometric measurements, and color pattern. A detailed morphological description of these specimens is provided in the Taxonomy section below.

Advertisement call comparisons. Advertisement calls of the two *Phyzelaphryne* males recorded at PNJ were composed of two pulsed notes, containing two, three or four pulses each (Fig. 4). Calls were emitted between irregular silent intervals (2.05–8.94 s), at an average peak frequency of 3.90 kHz and average lower and upper frequencies of 2.91 and 4.52 kHz, respectively. A second harmonic is visible on the spectrogram at about 7.50 kHz. Mean call duration was 0.053 s. Values of spectral and temporal traits of the first and second notes greatly overlapped but the first note was usually longer than the second and emitted with a lower peak frequency (Table 3). The two notes constituting a call were separated by a short silent interval, with mean duration of 0.018 s.

Advertisement calls of a male *Phyzelaphryne miriamae* recorded at Cachoeira do Teotônio, Rondônia were very similar to those recorded in PNJ, formed by two pulsed notes, containing two or three pulses each (Fig. 4). Silent intervals between calls varied between 4.2–8.2 s. Mean peak, lower and upper frequencies of calls were 3.76, 2.93 and 4.47 kHz, respectively. Mean call duration was 0.043 s. Values of spectral and temporal traits of the first and second notes overlapped (Table 3). The two notes were separated by a short silent interval, with mean duration of 0.020 s. Considering their range of variation, all call parameters analyzed overlapped between calls of *Phyzelaphryne* from PNJ and Rondônia.

Taxonomy

Based on the results of phylogenetic, morphological and acoustic analyses described above, specimens from PNJ and Floresta Nacional de Pau-Rosa are assigned to *Phyzelaphryne miriamae.* Accordingly, we provide an updated definition for the species, extend its geographic distribution, and report new observations on natural history and bioacoustics. Specimens from EEJJ are assigned to a new species of *Phyzelaphryne* that we describe below.

Phyzelaphryne miriamae Heyer, 1977

Figures 3, 4

Holotype. Adult female (MZUSP 49894) in good state of preservation after 43 years preserved in ethanol 70 %. Examination of the specimen revealed no incongruences or noteworthy variations when compared with the description of Heyer (1977) or with illustrations provided in Hoogmoed & Lescure (1984).

Amended definition. Heyer (1977) provided a common definition for *Phyzelaphryne* and *Phyzelaphryne miriamae*, assuming the genus was monospecific. Here, we amend the original definition of *P. miriamae*, highlighting traits that are useful for the species diagnosis relative to a new *Phyzelaphryne* species, described below.

Phyzelaphryne miriamae is characterized by: (1) small body size, males 14.6–16.2 mm, females 19.4–20.0 mm SVL; (2) skin on dorsum shagreened; ventral surfaces smooth, finely tuberculate only on ventral surface of thighs; (3) snout subacuminate in dorsal view, protruding in lateral view; (4) tympanum round, horizontal tympanum diameter approximately 40 % the diameter of eye; tympanic annulus complete; (5) subtympanic glandular ridge present from below tympanum to approximately the insertion of upper arm; (6) three round supernumerary tubercles on palmar surface, all similar in shape and only slightly variable in maximum diameter; (7) thenar tubercle and subarticular tubercle on finger I not fused, separated by a conspicuous gap; (8) inner metatarsal tubercle and subarticular tubercle of toe I not fused, separated by a short but conspicuous gap; (9) body coloration cryptic, dorsum uniformly brown, sometimes with scattered small cream blotches or dots, more dense on dorsal surfaces of limbs and snout; venter light brown with tiny cream spots, uniformly scattered on throat, chest and abdomen; (10) iris golden copper with black reticulations and bright red pupil ring.

Color in life. Based of digital photographs of specimens from PNJ and Rondônia (Fig. 4). Dorsum uniformly brown, with sparsely scattered small white dots, more densely scattered on snout. White spots sometimes present on upper and lower lips. Subtympanic glandular ridge white. Flanks brown, similar to dorsum, becoming paler

towards venter. Lateral surface of snout brown, darker than dorsal snout. Ventral surfaces of throat, chest, abdomen and limbs uniformly light gray, with uniformly scattered tiny white spots.

Dorsal surface of upper arm orange to yellow, peppered with brown melanophores. Dorsal surface of forearm brown with irregular yellow blotches. Dorsal surface of hand and fingers brown with irregular gray blotches. Dorsal surface of thigh and shank brown, same color as dorsum. Tarsal region brown with irregular yellow blotches. Dorsal surface of foot and toes brown with irregular gray blotches.

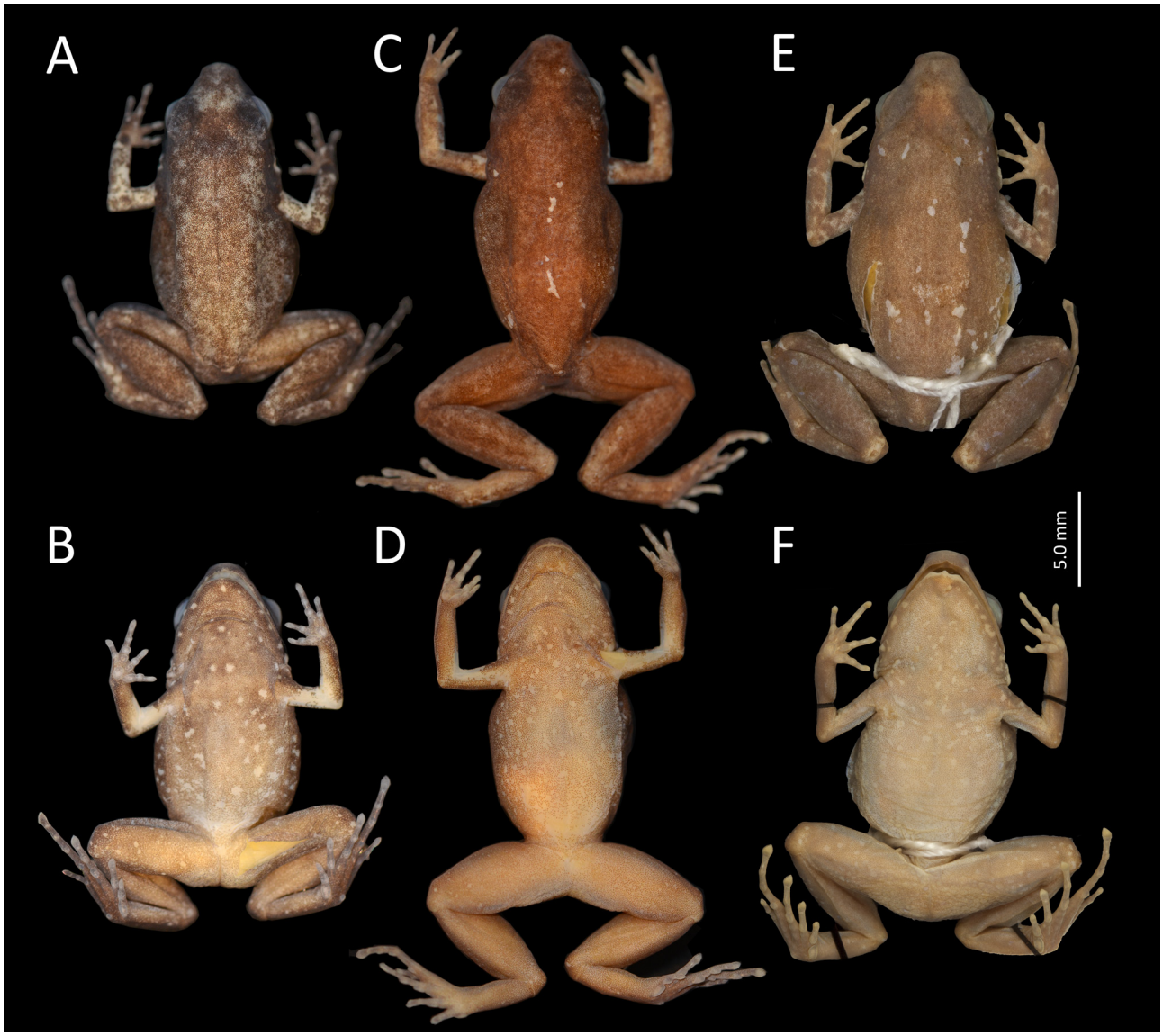

FIGURE 3. Dorsal and ventral views of preserved specimens of *Phyzelaphryne miriamae* from different localities in Brazil. (A, B) an adult male (MPEG 41043) from Parque Nacional do Jaú, state of Amazonas; (C, D) an adult male (MPEG 52025) from Floresta Nacional do Pau-Rosa, Coari, state of Amazonas; (E, F) holotype adult female (MZUSP 49894) from Igarapé Puruzinho, on the west bank of the Madeira River, state of Amazonas.

Advertisement call. The advertisement call of *Phyzelaphryne miriamae* consists of two or three pulsed notes, each note formed by 2–4 pulses. Call duration 0.041 to 0.059 s. Peak frequency of first note 3.53 to 4.07 kHz and its duration 0.014 to 0.023 s. Peak frequency of second note 3.53 to 4.09 kHz and its duration 0.012 to 0.022 s. Notes within a call are separated by a short silent interval, between 0.014–0.022 s long.

It is important to note that the advertisement call described and illustrated in Heyer (1977) actually belonged to *Adelophryne adiastola*, later described by Hoogmoed & Lescure (1994) from the reexamination of specimens considered in Heyer (1977).

Geographic distribution. Based on the new occurrences reported here for our study areas, *Phyzelaphryne miriamae* is distributed in the Madeira, Purus, Jaú and Solimões river basins west of Maués, Amazonas, Brazil. Its

easternmost record is 3.94711° S, 58.45627° W. Its western and southernmost record is in Cachoeira do Teotônio, Porto Velho, Rondônia, 8.82861° S, 64.074722° W, but the species is known to occur along most of the upper Madeira River (Santo Antônio Energia / Instituto Nacional de Pesquisas da Amazônia, *Estudos Ambientais no Rio Madeira, no trecho Cachoeira de Santo Antônio*, unpublished report available at http://licenciamento.ibama.gov.br/Hidreletricas/Santo%20Antonio%20(Rio%20Madeira)/ Relatorios/). Specimens collected in PNJ represent the northernmost record of the species, and the only record north of the Solimões/Amazon River (Fig. 1).

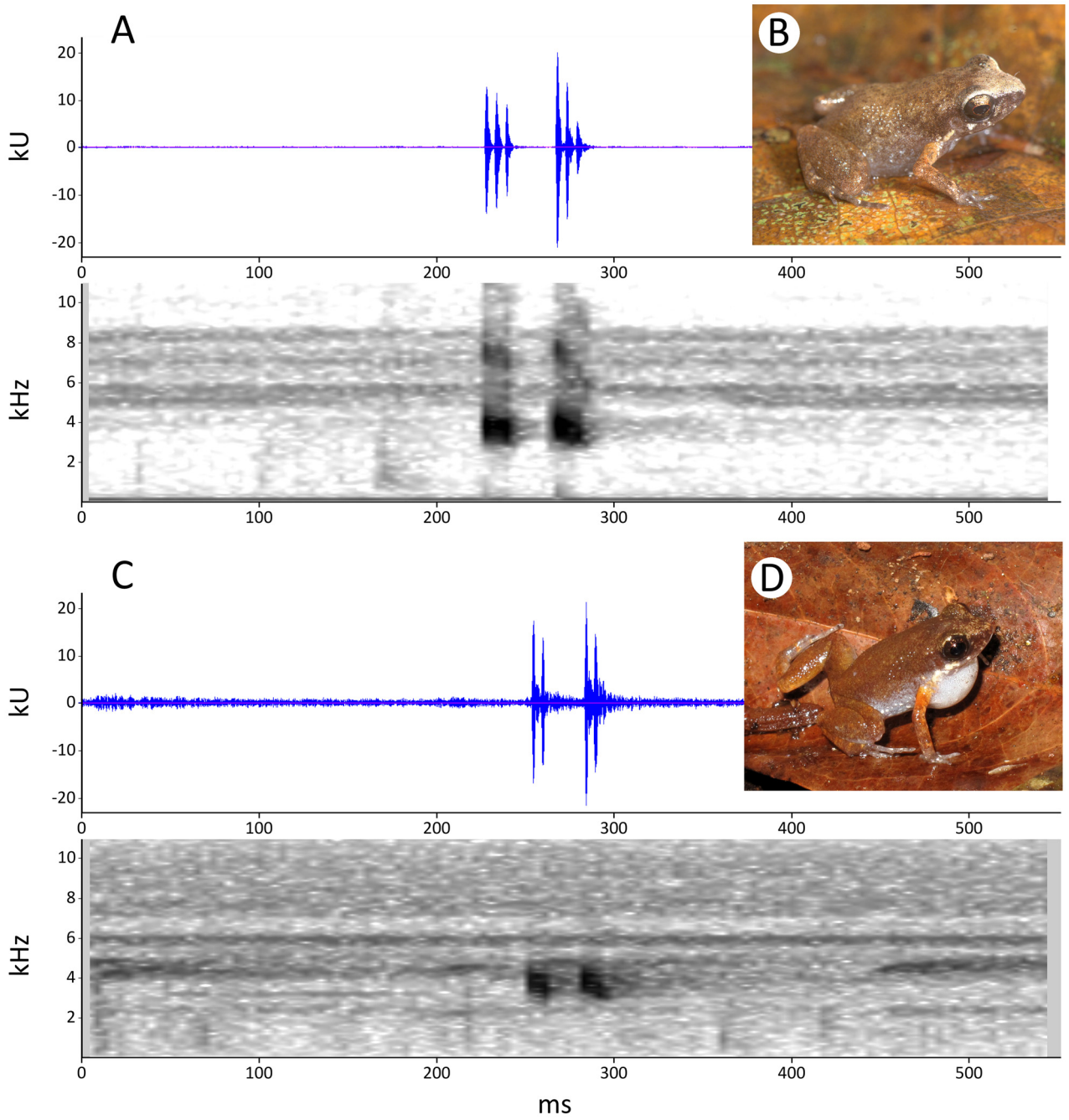

FIGURE 4. (A) Waveform (upper graph) and spectrogram (lower graph) of the advertisement call of a male *Phyzelaphryne miriamae* (MPEG 41045) recorded at Parque Nacional do Jaú (PNJ), Amazonas, Brazil. At PNJ, calls of *P. miriamae* are formed by two very short notes, containing four or three pulses each (three pulses each in this example). Note second harmonic with low sound intensity at approximately 7.5 kHz. (B) Photograph of a male (MPEG 41043) collected at the same locality. (C) Waveform and spectrogram of the advertisement call of a male of *P. miriamae* recorded in Cachoeira do Teotônio, Rondônia, on the left bank of the Madeira River, approximately 190 km southwest of the species type locality. These advertisement calls are formed by two very short notes, containing two or three pulses each (two pulses each in this example). (D) Photograph of the recorded male.

Natural history notes. At PNJ, male *Phyzelaphryne miriamae* were found calling, hidden in the leaf litter. Calling activity began at dusk and continued for several hours. Males were calling but most ceased calling once approached, which made them difficult to locate. Once located, males could be easily exposed by removal of a few leaves.

***Phyzelaphryne nimio* sp. nov.**
Figures 5–10, 12

Holotype. MCP 13719 (field code SCF 1846). An adult female, collected by G. Gagliardi-Urrutia, F.J.M. Rojas-Runjaic, P.I. Simões and S. Castroviejo-Fisher on 5 February 2017, in an area of *terra-firme* forest on the west bank of the Juami River (Canal da Inveja), within Estação Ecológica Juami-Japurá, state of Amazonas, Brazil (1.75834° S, 67.61532° W; ~ 67 m a.s.l.).

Paratypes. Thirty-three adult specimens, 16 females and 18 males. Females: MCP 13683–13697, 13720 (field codes SCF 1877, 2003, 1968, 1969, 1967, 1973, 1907, 1775, 1972, 1970, 1908, 1875, 1820, 1743, 1847, 1971, respectively). Males: MCP 13698–13715 (field codes SCF 1910, 1959, 1909, 1964, 1974, 1965, 1912, 1744, 1745, 1961, 1962, 1960, 1849, 1966, 1876, 1848, 1742, 1911, respectively). All collected by G. Gagliardi-Urrutia, F.J.M. Rojas-Runjaic, P.I. Simões and S. Castroviejo-Fisher between 2–9 February 2017 at the same site as the holotype and at a second sampling site within EEJJ (Igarapé da Fartura), on the east bank of the middle course of the Juami River (1.96063° S, 67.93694° W, ~ 71 m a.s.l.).

Referred specimens. MCP 13716, 13717 and 13718 (field codes SCF 1913, 1963 and 1978 respectively), all juvenile specimens, collected at Igarapé da Fartura sampling site, between 6–8 February 2017, same collectors as the paratypes. MCP 13725 (field code SCF 1975), three eggs laid by female paratype MCP 13688 on 08 February 2017.

Etymology. The specific epithet *nimio* is a Spanish masculine adjective derived from the Latin word *nimius* ("abundant" or "plentiful"). The Spanish term keeps this meaning but has also received the additional meaning of "insignificant" and "very small" (Real Academia Española 2014). The dual meaning of *nimio* alludes simultaneously to the abundance of the new species in the two localities where it was collected and to its very small body size, and is used in apposition to the genus.

Generic placement. We assign this new species to *Phyzelaphryne* based on its phylogenetic position using molecular data, and on the presence of the following diagnostic phenotypic characters, proposed by Hoogmoed & Lescure (1984): (1) Digits round in cross section; (2) discs on fingers and toes small, not expanded to moderately expanded, pointed at their tips; (3) discs of fingers III and IV and discs of toes I–V with distinct lateral grooves, interrupted only at the tip; (4) number of phalanges in fingers I–IV: 2-2-3-3; (5) number of phalanges in toes I–V: 2-2-3-4-3; (6) terminal phalanges in most fingers and toes with T-shaped tips; (7) tongue with a narrow anterior stem, widening into a large subcircular shape posteriorly; (8) a well-defined oblique subtympanic glandular ridge, not in contact with the tympanic annulus; (9) inguinal black spot absent.

Definition. *Phyzelaphryne nimio* is characterized by: (1) small body size, males 11.2 to 15.2 mm and females 13.2 to 15.9 mm in SVL; (2) skin on dorsum shagreened; ventral surfaces smooth, finely tuberculate only on thighs; (3) snout sub-acuminate in dorsal view, protruding in lateral view; (4) tympanum round and small, horizontal diameter approximately 30 % of eye diameter; tympanic annulus concealed dorsally by a skin fold; (5) subtympanic glandular ridge present from the mouth rictus to approximately the insertion of upper arm; (6) two or three pentagonal, trapezoid or ellipsoid supernumerary tubercles of which the one at the base of finger III is much larger than the others; (7) when conspicuous, supernumerary tubercle at the base of finger IV is ellipsoid, fused laterally with tubercle at the base of finger III; (8) thenar tubercle fused with subarticular tubercle on finger I; (9) inner metatarsal tubercle fused with subarticular tubercle of toe I; (10) cryptic body coloration, background color of dorsum tan or dark brown with darker brown mottling and small light brown or white spots, flanks tan or dark brown with white or light cream spots, ventral surfaces of body and limbs grayish brown, darkest on chest, with white blotches or spots; (11) iris golden copper with black reticulations and a bright red pupil ring.

Description of holotype. Adult female (SVL = 15.3 mm) in good state of preservation, with a piece of muscle ventrally cut from the right thigh and preserved as tissue sample (Fig. 5). Measurements of the holotype are in Table 1. Body robust, head wider than long (HL/HW = 0.9), head length 0.3 times the SVL. Eye length greater than

distance from anterior corner of eye to nostril (EN/EL = 0.7). Nares located posterolaterally to tip of snout, directed laterally. Nares opening laterally, visible in lateral view, but not distinct in ventral or dorsal views. Internasal distance 0.3 times HW. Snout sub-acuminate in dorsal view, protruding in lateral view. Canthus rostralis distinct, sharply angular from anterior corner of the eye to nostril, rounded from nostril to tip of snout. Loreal region slightly concave. Interorbital distance only slightly greater than internasal distance (IO/IN = 1.1). Distance between orbits 1.1 times the maximum width of eyelids, when measured dorsally (Fig. 5). Tympanum round, 0.3 times maximum length of eye. Tympanum distinct to the naked eye, tympanic annulus present, well-defined, one fourth of right tympanum concealed posterodorsally (Fig. 6), one third of left tympanum concealed dorsally.

FIGURE 5. Dorsal and ventral views of preserved specimens of *Phyzelaphryne nimio* **sp. nov.** Left: Holotype adult female (MCP 13719). Right: Paratype adult male (MCP 13715).

FIGURE 6. Lateral view of type specimens of *Phyzelaphryne nimio* **sp. nov.** Top: Holotype adult female (MCP 13719). Bottom: Paratype adult male (MCP 13715).

Tympanum separated from posterior corner of the eye by a distance of 0.5 times the maximum horizontal diameter of tympanum. Subtympanic glandular ridge present from the mouth rictus to approximately the insertion of the upper arm. Subtympanic glandular ridge not contacting the tympanic annulus. Anterior 25 % of tongue attached to the mouth floor, forming a narrow stem. Tongue widening into a subcircular shape posteriorly. Choanae round, positioned anteriorly to prevomerine processes and eye bulge. Dentigerous processes straight, not in contact, sharply separated, forming a transverse row, located between the choanae and the eye bulge. Vomerine teeth present, not visible under maximum (60 X) magnification but detectable by moving a wire probe along the vomerine surface.

Lengths of upper arm and forearm 0.2 and 0.3 times the SVL. Palmar tubercle round to slightly elliptical. Thenar tubercle present, oval, slightly pointed distally, fused with subarticular tubercle of finger I. Maximum diameter of thenar tubercle 62 % of maximum diameter of palmar tubercle (Fig. 7). Three supernumerary tubercles present at the bases of fingers II, III and IV. Supernumerary tubercle at the base of finger III pentagonal, about the same diameter as palmar tubercle, 1.3 times size of pentagonal supernumerary tubercle at the base of finger II. Supernumerary tubercle at the base of finger IV small, ellipsoid, flat and fused laterally with supernumerary tubercle at the base of finger III. Subarticular tubercles on fingers I to IV one, one, two and one respectively. Subarticular tubercles generally round, protuberant, slightly exceeding the width of phalanges. Subarticular tubercle on finger I elliptical, distally acuminate. Fingers unwebbed. Tip of Finger IV reaching the center of distal subarticular tubercle of Finger III when fingers are juxtaposed. Relative lengths of fingers: IV < II = I < III. Fingers with mucronate, abruptly pointed tips. Discs of fingers I and II not expanded, never exceeding the width of phalanges. Discs of fingers III and IV weakly expanded, width of discs corresponding to 1.0 and 1.1 times the width of their respective adjacent phalanges (Fig. 7).

Tibia length half SVL (TL/SVL = 0.5). Keels or tubercles absent on tarsal region. Inner metatarsal tubercle elliptical, fused with subarticular tubercle of toe I. Outer metatarsal tubercle small and round, its maximum diameter equal to 0.4 of maximum diameter of inner metatarsal tubercle (Fig. 8). Metatarsal region smooth, with no folds, ridges or additional tubercles. Toes unwebbed. Relative lengths of toes I < II < V < III < IV. Toes with mucronate, abruptly pointed tips. Discs of toes I and V not expanded, not exceeding the width of adjacent phalanges. Discs of toes II, III and IV moderately expanded, width of discs 1.1, 1.4 and 1.6 times the width of adjacent phalanges. One, one, two, three and two subarticular tubercles are present on toes I to V, respectively. Dorsal skin shagreened. Ventral skin smooth, finely tuberculate only medially on thigh.

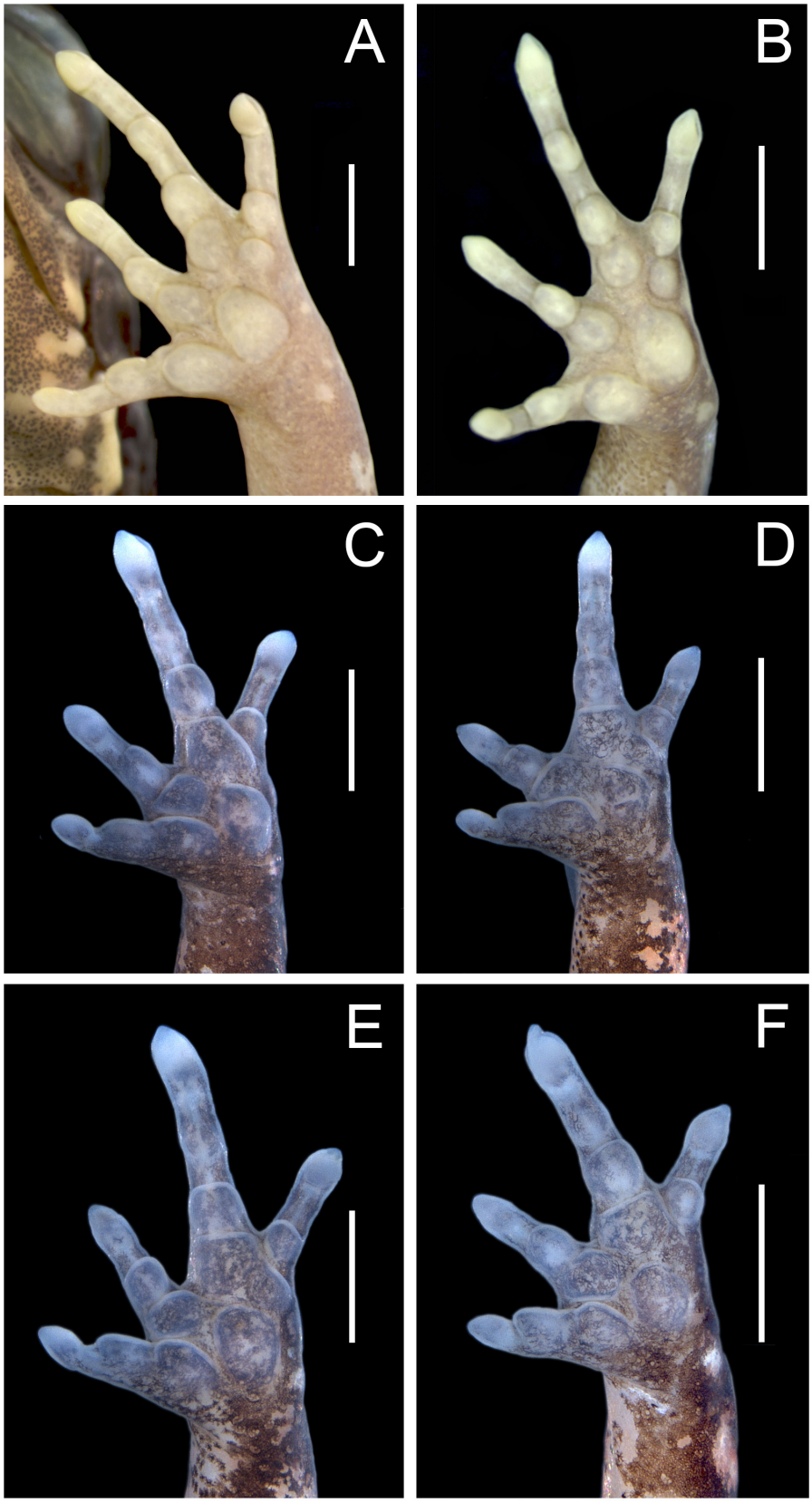

FIGURE 7. Ventral view of the left hand of preserved type specimens of *Phyzelaphryne miriamae* (A, B) and *P. nimio* **sp. nov.** (C–F). (A) Holotype adult female (MZUSP 49894). (B) Paratype adult male (MZUSP 49895). (C) Paratype adult female (MCP 13691). (D) Paratype adult male (MCP 13715). (E) Holotype adult female (MCP 13719). (F) Paratype adult male (MCP 13711). Scale bars = 1.0 mm.

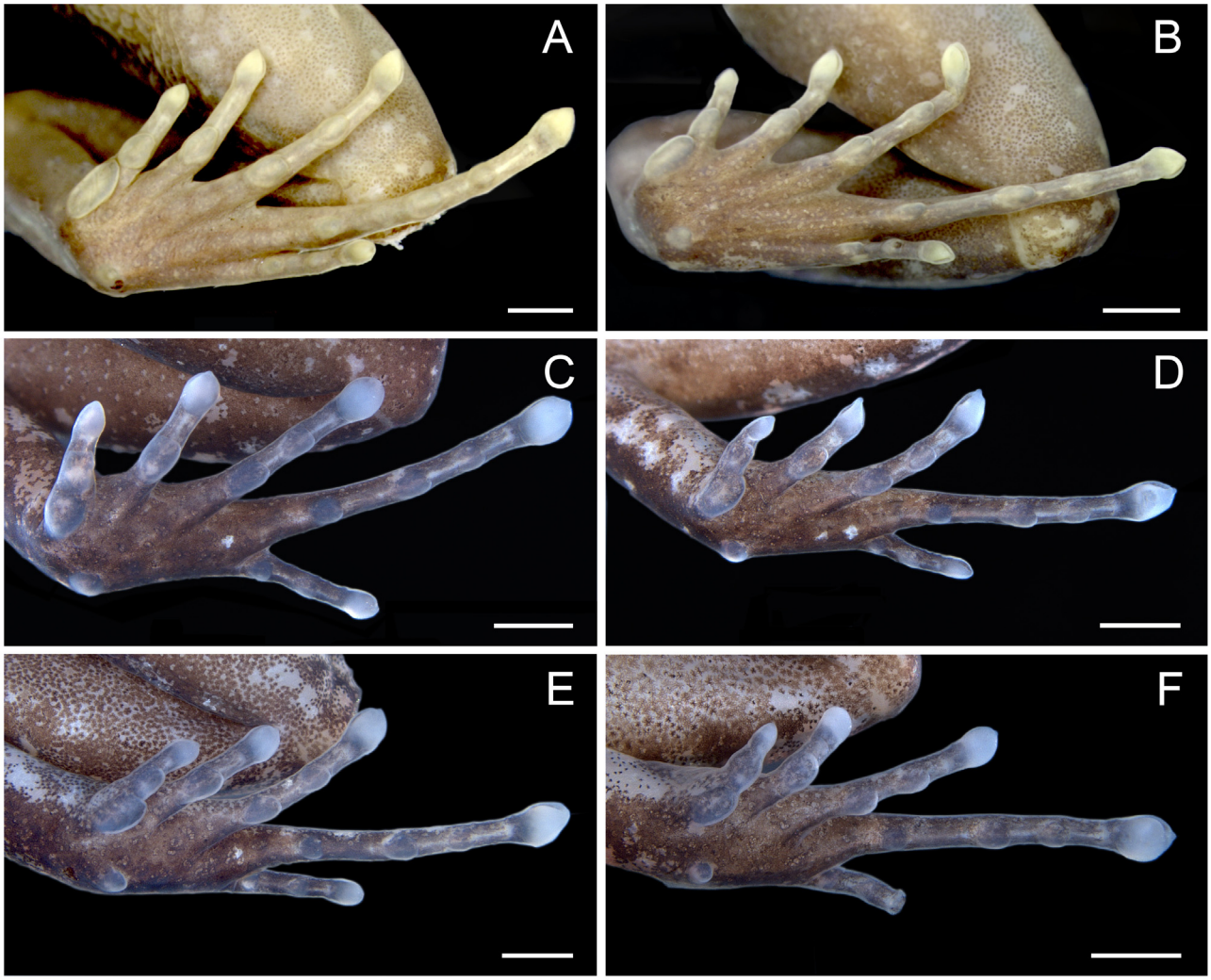

FIGURE 8. Ventral view of the left foot of preserved type specimens of *Phyzelaphryne miriamae* (A, B) and *P. nimio* **sp. nov.** (C–F). (A) Holotype adult female (MZUSP 49894). (B) Paratype adult male (MZUSP 49895). (C) Paratype adult female (MCP 13691). (D) Paratype adult male (MCP 13711). (E) Holotype adult female (MCP 13719). (F) Paratype adult male (MCP 13715). Scale bars = 1.0 mm.

Color of holotype in preservative. Dorsum tan brown with scattered irregular dark brown spots and mottling. Dorsum grayish dark brown on supraorbital region and laterally, from snout to shortly posterior to the level of upper arm insertion (Fig. 5). Flanks the same color pattern as dorsum, with large dark brown areas from tip of snout to anterior corner of the eye, from posterior corner of the eye to shortly posterior to upper arm insertion (above tympanum and upper arm insertion) and on inguinal region (Fig. 6). A transverse pale stripe is present ~ 1.5 mm posterior to upper arm in right lateral view. The same region is uniformly dark brown in left lateral view. Upper and lower lips with irregular white blotches, larger at the level of the eye than anteriorly. White blotches appear ventrolaterally, merging with color pattern of abdomen. Ventral surfaces with cream round marks on brown background. Density of melanophores variable longitudinally, rendering the brown background to be lighter on throat and abdomen and darker on chest (Fig. 5). Tongue is pale cream.

Arm pale cream with irregular dark brown blotches along their outer edge and on wrist in dorsal view. Hand pale cream, with brown areas on proximal dorsal surface of metacarpal region and on fingers. Tips of fingers brown, Finger III pale brown at tip. Ventral upper arm pale cream to translucent with a few melanophores scattered laterally. Forearm brown with pale cream blotches ventrally. Carpal and metarcarpal regions gray to translucent, with scattered brown pigments visible through skin in ventral view (Fig. 7).

Area immediately around vent uniform dark brown. A pale transverse bar flanks the dark brown area surrounding vent on the proximal region of thigh, in posterior view. Dorsal surface of thigh tan brown with dark

brown marks forming incomplete transverse bars. Thigh ventrally light brown with cream round marks. Inner and outer lateral surfaces of thigh dark brown with pale cream dots. Dorsal surface of shank same color as thigh, with larger irregular dark brown blotches present medially. Ventral surface of shank uniformly tan. Dorsal surface of tarsal region and foot same color as dorsal surface of shank. Tarsal and palmar regions dark brown with a few pale cream blotches. In dorsal view, toes with an alternating dark brown/pale cream pattern. Toes uniformly dark brown in ventral view (Fig. 8).

Osteology of fingers and toes. From examination of cleared and stained female paratype (MCP 13720), the number of phalanges in fingers I–IV of *Phyzelaphryne nimio* are 2-2-3-3, respectively (Fig. 9). Tips of terminal phalanges of fingers II, III and IV are T-shaped. Tip of terminal phalanx of finger I is blunt. The number of phalanges in toes I–V are 2-2-3-4-3 (Fig. 9). Tip of terminal phalanges of all toes are T-shaped.

FIGURE 9. Dorsal view of the cleared and stained hand (top) and ventral view of foot (bottom) of a female paratype (MCP 13720) of *Phyzelaphryne nimio* **sp. nov.** Note T-shaped tips of terminal phalanges on fingers II, III and IV and toes I–IV. Tip of toe V is indistinct in this view, but it is also T-shaped.

Variation in type series. Variation in morphometric measurements of female and male types are presented in Table 1. SVL of females generally larger than males (female SVL: mean = 13.2 mm, range 13.2–15.9; male SVL: mean = 12, range = 11.2–15.2). SVL of three juvenile specimens for which sex could not be determined were 10.7, 10.7 and 10.5 mm. Body proportions of adults (HL/SVL, HW/SVL, HL/HW, SL/SVL, TYM/SVL, FAL/SVL, TL/SVL) overlapping between sexes.

Canthus rostralis in cross section varying from angular to nearly rounded between anterior corner of the eye to nostril in cross section, concave in dorsal view. Vocal sac of males subgular, single and small, not extending onto chest or arm insertion (Fig. 5), sometimes forming wrinkles on the surface of throat. Vocal slits flanking tongue at its posterior third, with darkly pigmented borders. Dentigerous process slightly convex in specimens MCP 13690

and MCP 13715. One third of tympanum dorsally concealed in 65 % and one fourth of tympanum dorsally concealed in 35 % of specimens.

Supernumerary tubercle at the base of finger IV conspicuous in all female specimens and in 50 % of male specimens, inconspicuous in the remaining males. When conspicuous, supernumerary tubercle at the base of finger IV is fused with the one at the base of finger III. Supernumerary tubercles pentagonal or trapezoid (Fig. 7).

Color in life. Description is based on field observations and photographs of specimens forming the type series. Coloration is variable among type specimens, but not sexually dimorphic (Fig. 10). Juvenile specimens have the same color pattern as adults.

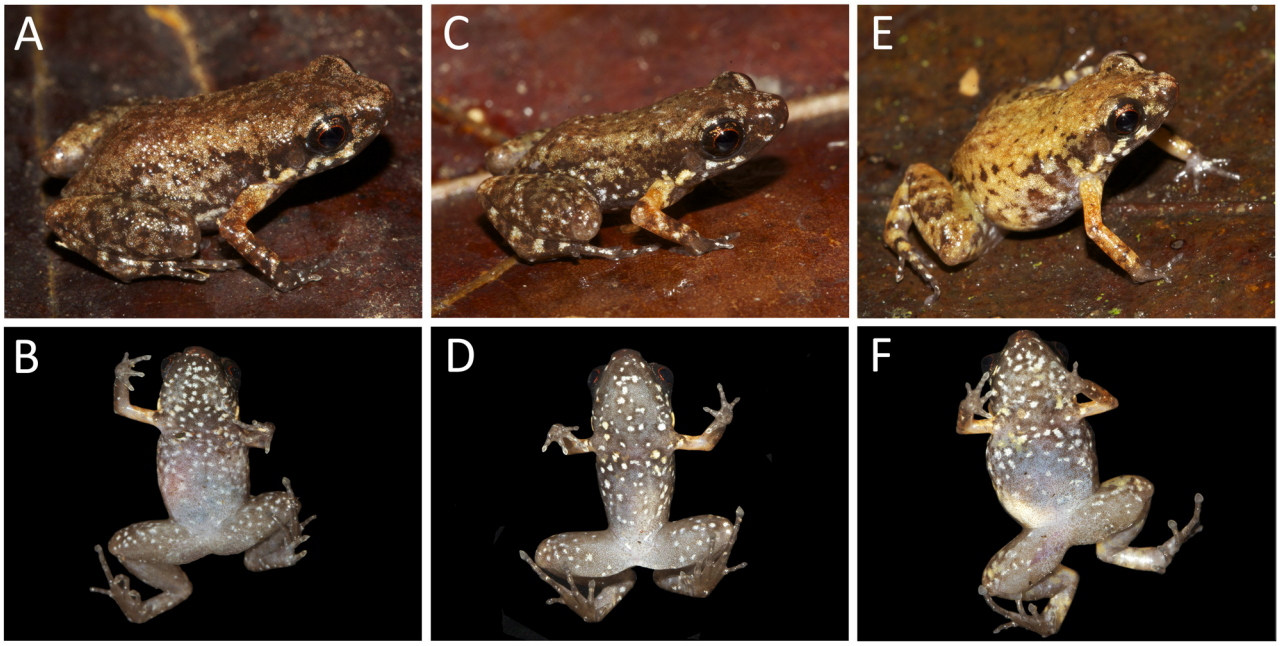

FIGURE 10. Color variation in life in *Phyzelaphryne nimio* **sp. nov.** (A, B) Adult female paratype MCP 13696; (C, D) male paratype MCP 13714; (E, F) gravid female paratype MCP 13690, with egg visible through translucent skin on the posterior right flank (F).

Dorsum tan, brownish orange or brownish yellow, with variable dark brown mottling. Scattered small white dots present on dorsum in some individuals. Flanks same color as dorsum, with dark brown areas extending from behind the eye to above upper arm insertion. Large dark brown patches generally present ventrolaterally. Bright white spots present ventrolaterally on flanks and on upper and lower lips, generally more evident below the eye. Lateral bright spots whitish yellow in some individuals. Venter grayish brown, darker anteriorly. Irregular bright white spots present on all ventral surfaces, dense on throat and chest, sparse on posterior abdomen. Spots frequently with a darker grayish brown margin.

Dorsal surface of upper and forearm dark yellow with dark brown mottling, denser on forearm. Isolated bright white spots sometimes present on dorsal surface of forearm. Ventral surface of upper arm yellow to translucent. Forearm, carpal and metacarpal regions and fingers gray ventrally, gray with bright white spots dorsally.

Area immediately adjacent to vent uniform dark brown. Inner lateral surface of thigh dark brown with scattered irregular white spots, varying in shape, size and density among individuals. Dorsal surfaces of thigh and shank same color as dorsum, generally with dark brown mottling, sometimes forming irregular transverse dark brown bars. Venter of thigh grayish brown with bright white spots, same color as anterior ventral surfaces of body. Ventral surface of shank solid grayish brown. Dorsal surface of tarsal region same color as thigh and shank, with alternating transverse pale (tan brown, light brown or white) and dark brown blotches. Ventral surfaces of tarsal and plantar regions solid dark gray in ventral view. Toes with alternating transverse white and dark brown blotches ventrally. Iris is golden copper with black reticulations and a bright red pupil ring.

Natural history. *Phyzelaphryne nimio* is a very small nocturnal and hemiedaphic frog that inhabits the leaf litter of *terra-firme* rainforests (Fig. 11) at EEJJ. None were detected in flooded forest areas or at channel or river edges. The species is very abundant at the two localities where it was collected (Canal da Inveja and Igarapé da

Fartura), but can go unnoticed due to its secretive habits, small size and cryptic coloration. When leaf litter is removed and they jump to escape, they can be easily mistaken for crickets. Despite their small size their jumps can reach approximately one meter, more than 60 times their mean SVL. *Phyzelaphryne nimio* was hardest to detect during nocturnal searches after a rain; the largest numbers of individuals were detected on dry nights. We detected a high number of specimens during our nocturnal surveys by careful removal of leaf litter using feet or sticks. *Phyzelaphryne nimio* was more abundant in areas where the forest floor was covered by a deep layer of leaf litter, ca. 25–40 cm. At least 15 specimens were detected by leaf litter removal with a stick in about 20 minutes in an area of *ca*. 10 m^2, near the basecamp of Igarapé da Fartura at 22:00 h on 08 February 2017. In spite of the abundance of this species and the great sampling effort at the two localities, no calling males were detected. At least eight of the adult females collected were ovate (MCP 13684, 13686, 13687, 13688, 13690, 13691, 13692, 13720); two or three very large eggs were evident through the translucent skin on their flanks. An amplectant couple (male MCP 13702; female MCP 13688; Fig. 12) was found in cephalic amplexus on the leaf litter at 22:10 h on 08 February 2017 in the vicinity of the basecamp of Igarapé da Fartura. During transport to the camp, the female laid three large eggs on the leaf litter in the transporting bag. Eggs were 3.9, 4.0 and 4.3 mm in maximum diameter and their yolk was uniformly white (Fig. 12). Juveniles were very uncommon in our sample, with only three juvenile specimens collected (MCP 13716, 13717 and 13718).

FIGURE 11. (A) Canal da Inveja, a black water watercourse at Estação Ecológica Juami-Japurá (EEJJ), state of Amazonas, Brazil. In this conservation unit, *terra-firme* forests such as the type locality of *Phyzelaphryne nimio* **sp. nov.** are accessed from water channels and creeks. (B) Habitat of *P. nimio* at EEJJ.

Diagnosis. Because *Phyzelaphryne* and *Adelophryne* share a very similar external morphology, we compare the new species with all currently recognized Amazonian Phyzelaphryninae. Character states in species other than *P. nimio* are described in parentheses.

Phyzelaphryne nimio is most easily distinguished from *Phyzelaphryne miriamae* Heyer, 1977 by the morphology of the carpal and metacarpal ventral surfaces. *Phyzelaphryne nimio* differs from *P. miriamae* by the presence of three pentagonal, trapezoid or ellipsoid supernumerary tubercles (three round to elliptical supernumerary tubercles in *P. miriamae*). Supernumerary tubercle at the base of finger III 1.3–1.4 times larger in maximum diameter than the supernumerary tubercles at the base of fingers II or IV, respectively (supernumerary tubercles only slightly variable in maximum diameter). Supernumerary tubercle at the base of finger IV not protuberant, sometimes inconspicuous (supernumerary tubercle at the base of finger IV protuberant, always conspicuous). When conspicuous, supernumerary tubercle at the base of finger IV is fused with tubercle at the base of finger III (supernumerary tubercles separated by a conspicuous gap). Thenar tubercle fused with subarticular tubercle on finger I (thenar tubercle and subarticular tubercle on finger I separated by a conspicuous gap). Inner

metatarsal tubercle and subarticular tubercle of toe I fused (inner metatarsal tubercle and subarticular tubercle of toe I not fused, separated by a short, but conspicuous gap). Male *P. nimio* generally smaller than male *P. miriamae,* although the ranges of their SVL overlap (male *P. nimio* = 11.2–15.2 mm; male *P. miriamae* 14.6–16.2 mm). Female *P. nimio* much smaller than female *P. miriamae* (SVL range in female *P. nimio* 13.2–15.9 mm; SVL range in female *P. miriamae* 19.4–20.0 mm).

FIGURE 12. (A) Cephalic amplexus of *Phyzelaphryne nimio* **sp. nov.** male paratype MCP 13702 (SVL = 11.9 mm) and female paratype MCP 13688 (SVL = 14.0 mm). (B) Eggs laid by MCP 13688. Diameter of eggs ranged between 3.9 and 4.3 mm.

Phyzelaphryne nimio differs from all Amazonian species of *Adelophryne* in having cylindrical digits in cross section (digits flattened), by the presence of distinct, round subarticular tubercles on fingers (indistinct subarticular tubercles), by having a large subcircular tongue (tongue narrow, not expanding into a subcircular shape posteriorly) and by the presence of a small subgular vocal sac, indistinct in preserved male specimens (subgular vocal sacs large, conspicuous as skin folds, commonly extending to the level of chest or that of the upper arm insertion). It also differs in having tympanum separated from eye by a distance much less than the maximum horizontal diameter of tympanum (tympanum separated from eye by a distance equal to or slightly less than horizontal diameter of tympanum).

Phyzelaphryne nimio differs from *Adelophryne adiastola* Hoogmoed & Lescure, 1984 in having three phalanges on finger IV (two phalanges on finger IV), in having white or cream spots on flanks (white or cream spots absent on flanks) and in having a brown dorsum with dark brown mottling and with small cream or white spots (dorsum uniformly brown).

Phyzelaphryne nimio differs from *Adelophryne gutturosa* Hoogmoed & Lescure, 1984 in having tips of fingers III and IV weakly expanded into discs (no discs on tips of fingers) and by venter grayish brown, darkest on chest, with scattered white spots (venter dark brown, darkest on throat, with small white dots).

Phyzelaphryne nimio differs from *Adelophryne patamona* MacCulloch, Lathrop, Kok, Minter, Khan & Barrio-Amorós, 2008 by ventral color in life: grayish brown, darker on chest, with irregular bright white spots dense on throat and chest, sparse on posterior abdomen (throat, chest and underside of upper arms dark gray with white or pale blue spots; posterior abdomen and underside of legs reddish brown with white or pale blue spots).

Geographic distribution. *Phyzelaphryne nimio* is currently known from *terra-firme* forests in the Juami River basin, south of the Japurá River, Amazonas, Brazil (Fig.1). Two other nearby sites were searched: 1) riverside environments and on small islands at the confluence of Juami and Japurá rivers (1.73946° S, 67.60149° W, 44 km from the type locality, and 2) north bank of the Japurá River (Comunidade de Barreirinha, 1.64137° S, 67.70606° W, 43 km from type locality). No specimens of *P. nimio* were found in these locations.

Discussion

Phyzelaphryne nimio is the first species in the genus to be described in over 40 years, demonstrating the difficulty

of discovering the true diversity of small frogs inhabiting the leaf litter in Neotropical rainforests. Recently, the paucity of taxa in Phyzelaphryninae and the geographically fragmented species records within this group have led researchers to hypothesize that it constitutes a relict clade, with extant taxa representing remnants of a once diverse and widely distributed evolutionary lineage (Gonzalez-Voyer *et al.* 2011). This view was challenged by the analyses of DNA sequences of a large series of specimens sampled across eastern and northern South America, which revealed the existence of several evolutionary lineages within *Phyzelaphryne* and *Adelophryne*, most of which remain unnamed (Fouquet *et al.* 2012). Our work contributes to these latter findings by revealing a previously undetected clade within *Phyzelaphryne*, by extending the known geographic distribution of *P. miriamae* and supporting the view that insufficient sampling is implicated in the presumed low species richness and fragmented geographic distribution of Phyzelaphryninae. We expect that fieldwork in areas previously unsampled for leaf litter-dwelling frogs in Amazonia will increase the number of species in this group, as well as provide us with a better understanding of their biogeography.

Phyzelaphryne was previously considered to be distributed in southern Amazonia, with the exception of a single record in Leticia, Colombia, on the north bank of the Amazonas River (Fouquet *et al.* 2012). The split between *Phyzelaphryne* and *Adelophryne* lineages was attributed to climatic events along the Eocene/Oligocene boundary (~ 27.4–40.5 Ma ago), which possibly fragmented continuous forest ranges between northern and southern Amazonia (Fouquet *et al.* 2012). Our results show that *Phyzelaphryne* is widely distributed north of the Amazonas/Solimões River, suggesting that other historical scenarios must be evaluated in order to uncover the historical factors associated with the divergence between the two main lineages of Phyzelaphryninae.

The geographic distribution of the species of *Phyzelaphryne*, including the two candidate species *Phyzelaphryne* sp. (C1) and *Phyzelaphryne* sp. (C2), is puzzling. Small, fossorial, direct-developing anurans are considered poor dispersers so one may expect small species ranges and marked phylogeographic patterns. This seems to be the case in *Adelophryne*, where phylogenetic analyses revealed that most of the genetically divergent clades are restricted to small areas (Fouquet *et al.* 2012). However, our data on *Phyzelaphryne* points to a different pattern. On one hand, *P. miriamae* has been recorded at localities separated by more than 1,000 km (Fig. 1) and by geographic barriers of the caliber of the Amazon and Madeira Rivers. On the other, it seems that *P. nimio* and *Phyzelaphryne* sp. (C2) may actually occupy considerably smaller areas, fitting the expected pattern for such small fossorial anurans. Although the knowledge of small leaf litter-dwelling frogs in the Amazon is very far from complete, the current pattern of *Phyzelaphryne*, with one species widely distributed and a few others restricted to much smaller areas, conforms to that exhibited by other more diverse genera such as *Osteocephalus* and *Ranitomeya* (Brown *et al.* 2011; Jungfer *et al.* 2013).

Phyzelaphryne miriamae and *P. nimio* are both found in well-preserved protected areas in Brazil. Although the population size and trends in both species are unknown, their conservation status currently benefits from the large areas of continuous forests contained within these reserves, as well as their remoteness. However, present (this study) and past (*i.e.*, Fouquet *et al.* 2012) phylogenetic analyses are unequivocal in identifying phylogenetic structure within *Phyzelaphryne miriamae* and in suggesting the existence of at least two additional putatively unnamed species of *Phyzelaphryne*. The taxonomic status of these populations must be addressed before effective planning for conservation can be traced for all of the phylogenetic lineages within *Phyzelaphryne.* Most of the phylogenetic diversity uncovered by these studies relate to specimens collected on the drainages of the Madeira, Purus and Abacaxis rivers, which are notoriously affected by contemporary developments such as river damming, roads, human settlements and forest logging (Fearnside & Graça 2006; Trancoso *et al.* 2009; Fearnside 2014; 2015). Hence, complementary approaches to amphibian species surveys, such as DNA-barcoding, should be included in environmental impact assessment studies in order to evaluate potential threats to *Phyzelaphryne* diversity at the regional scale.

Acknowledgements

We are grateful to Mauricio Rivera-Correa, Ross MacCulloch and one anonymous reviewer for the careful revision of the manuscript. We thank Taran Grant (MZUSP), Ana L. C. Prudente (MPEG) and Kevin de Queiroz (USNM) for granting us access to specimens under their care. We thank Maria Laura Delapieve, Bárbara Calegari, Juliano Romanzini and Tiffany M. da Silva for assisting us with staining and photographing specimens. We are grateful to

Ailton M. da Silva, Gutemberg M. Nascimento, José G. da Silva and Raimundo N. L. da Silva for field assistance at EEJJ. We are also thankful to the boat crew of "*Castelo Guedes III*" and fellow researchers (Lincoln Carneiro, Pablo Cerqueira, Pedro Dias, Hueliton Ferreira, Bernardo Santos and Níthomas Feitosa) for companionship and help during fieldwork at PNJ. We thank Elder Pena, Mariana Leitão and Josângela Jesus and all of the ICMBio staff in Tefé and Novo Airão for their invaluable logistical support. The expedition to EEJJ was funded by grants from Programa de Excelência Acadêmica of Coordenação de Aperfeiçoamento de Pessoal de Nível Superior (PROEX-CAPES, project #1030/2014), with additional funds from Programa de Áreas Protegidas of Instituto Chico Mendes de Conservação da Biodiversidade (ARPA/ICMBio). The expedition to PNJ was funded by the National Geographic Society (#WGS 430-16) and the Smithsonian Institution Global Genome Initiative. Acoustic data of *P. miriamae* were obtained with the support of Santo Antônio Energia S.A. Collection permits for both EEJJ and PNJ expeditions were provided by ICMBio and the respective park administration (permit numbers #57090-1 for EEJJ, #56338-1 for PNJ). PIS currently receives a post-doctoral fellowship from PNPD-CAPES through Programa de Pós-Graduação em Zoologia of PUCRS. PLVP was supported by a grant from Conselho Nacional de Desenvolvimento Científico e Tecnológico (CPNq BJT 313680/2014-0), JCLC was supported by Programa de Capacitação Institucional do Museu Paraense Emílio Goeldi (PCI/MPEG/MCTIC 312847/2015-7), MJS was supported by a scholarship from Coordenação de Aperfeiçoamento de Pessoal de Nível Superior. FJMRR and GGU are currently supported by PhD scholarships from CNPq (processes 142444/2014-6 and 140716/2016-5, respectively). This study was financed in part by the Coordenação de Aperfeiçoamento de Pessoal de Nível Superior - Brasil (CAPES) - Finance Code 001.

References

Andersson, L.G. (1945) Batrachians from East Ecuador, collected 1937, 1938 by Wm. Clarke-Macintyre and Rolf Blomberg. *Arkiv för Zoologi. Stockholm*, 37A (2), 1–88.

Benson, D.A., Cavanaugh, M., Clark, K., Karsch-Mizrachi, I., Lipman, D.J., Ostell, J. & Sayers, E.W. (2013) GenBank. *Nucleic Acids Research*, 41, 36–42. [D36–D42]
https://doi.org/10.1093/nar/gks119

Bioacoustics Research Program (2011) *Raven Pro: Interactive Sound Analysis Software. Version 1.4*. The Cornell Lab of Ornithology, Ithaca, New York. [software]

Brown, J.L., Twomey, E., Amézquita, A., Souza, M.B., Caldwell, J.P., Lötters, S., von May, R., Melo-Sampaio, P.R., Mejía-Vargas, D., Perez-Peña, P., Pepper, M., Poelman, E.H., Sanchez-Rodriguez, M. & Kyle Summers, K. (2011) A taxonomic revision of the Neotropical poison frog genus *Ranitomeya* (Amphibia: Dendrobatidae). *Zootaxa*, 3083, 1–120.

Duellman, W.E & Lehr, E. (2009) *Terrestrial-Breeding Frogs (Strabomantidae) in Peru*. Natur und Tier—Verlag Gmbh, Münster, 382 pp.

Farris, J.S., Albert, V.A., Källersjö, M., Lipscomb, D. & Kluge, A.G. (1996) Parsimony jackknifing outperforms neighbor-joining. *Cladistics*, 12, 99–124.?
https://doi.org/10.1111/j.1096-0031.1996.tb00196.x

Fearnside, P.M. (2014) Impacts of Brazil's Madeira River dams: Unlearned lessons for hydroelectric development in Amazonia. *Environmental Science & Policy*, 38, 164–172.
https://doi.org/10.1016/j.envsci.2013.11.004

Fearnside, P.M. (2015) Tropical hydropower in the clean development mechanism: Brazil's Santo Antônio Dam as an example of the need for change. *Climatic Change*, 131, 575–589.
https://doi.org/10.1007/s10584-015-1393-3

Fearnside, P.M. & Graça, P.M.L.A. (2006) BR-319: Brazil's Manaus-Porto Velho highway and the potential impact of linking the arc of deforestation to central Amazonia. *Environmental Management*, 38, 705–716.
https://doi.org/10.1007/s00267-005-0295-y

Felsenstein, J. (1985) Confidence limits on phylogenies: an approach using the bootstrap. *Evolution*, 39, 783–791.
https://doi.org/10.1111/j.1558-5646.1985.tb00420.x

Fouquet, A., Loebmann, D., Castroviejo-Fisher, S., Padial, J.M., Orrico, V.G.D., Lyra, M.L., Roberto, I.J., Kok, P.J.R, Haddad, C.F.B. & Rodrigues, M.T. (2012) From Amazonia to the Atlantic forest: Molecular phylogeny of Phyzelaphryninae frogs reveals unexpected diversity and a striking biogeographic pattern emphasizing conservation challenges. *Molecular Phylogenetics and Evolution*, 65 (2), 547–561.
https://doi.org/10.1016/j.ympev.2012.07.012

Frost, D. (2018) Amphibian Species of the World: an Online Reference. Version 6.0. American Museum of Natural History, New York. Available from: http://research.amnh.org/vz/herpetology/amphibia/ (accessed 17 May 2018).

Goloboff, P.A., Farris, J.S. & Nixon, K.C. (2008) TNT, a free program for phylogenetic analysis. *Cladistics*, 24, 774–786.

https://doi.org/10.1111/j.1096-0031.2008.00217.x
Gonzalez-Voyer, A., Padial, J.M., Castroviejo-Fisher, S., De La Riva, I. & Vilà, C. (2011) Correlates of species richness in the largest Neotropical amphibian radiation. *Journal of Evolutionary Biology*, 24 (5), 931–942.
https://doi.org/10.1111/j.1420-9101.2011.02243.x
Hedges, S.B., Duellman, W.E. & Heinicke, M.P. (2008) New World direct-developing frogs (Anura: Terrarana): Molecular phylogeny, classification, biogeography, and conservation. *Zootaxa*, 1737, 1–182.
Heinicke, M.P., Lemmon, A.R., Lemmon, E.M., McGrath, K. & Hedges, S.B. (2018) Phylogenomic support for evolutionary relationships of New World direct-developing frogs (Anura: Terraranae). *Molecular Phylogenetics and Evolution*, 118, 145–155.
https://doi.org/10.1016/j.ympev.2017.09.021
Heyer, W.R. (1977) Taxonomic notes on frogs from the Madeira and Purus rivers, Brasil. *Papéis Avulsos de Zoologia*, 31, 141–162.
Hoogmoed, M.S. & Lescure, J. (1984) A new genus and two new species of minute leptodactylid frogs from northern South America, with comments upon *Phyzelaphryne* (Amphibia: Anura: Leptodactylidae). *Zoologische Mededelingen Leiden*, 58 (6), 85–11.
Jungfer, K.H., Faivovich, J., Padial, J.M., Castroviejo-Fisher, S., Lyra, M.M., Berneck, B.V.M., Haddad, C.F.B., Iglesias, P.P., Kok, P.J.R., MacCulloch, R.D., Rodrigues, M.T., Verdade, V.K., Torres-Gastello, C.P., Chaparro, J.C., Valdujo, P.H., Reichle, S., Moravec, J., Gvoždík, V., Gagliardi-Urrutia, G., Ernst, R., De la Riva, I., Means, D.B., Lima, A.P., Señaris, J.C. & Wheeler, W.C. (2013) Systematics of spiny-backed treefrogs (Hylidae: *Osteocephalus*): An Amazonian puzzle. *Zoologica Scripta*, 42, 351–380.
https://doi.org/10.1111/zsc.12015
Katoh, K. & Standley, D.M. (2013) MAFFT Multiple Sequence Alignment Software Version 7: Improvements in Performance and Usability. *Molecular Biology and Evolution*, 30 (4), 772–780.
https://doi.org/10.1093/molbev/mst010
Kearse, M., Moir, R., Wilson, A., Stones-havas, S., Sturrock, S., Buxton, S., Cooper, A., Markowitz, S., Duran, C., Thierer, T., Ashton, B., Meintjes, P. & Drummond, A. (2012) Geneious Basic: an integrated and extendable desktop software platform for the organization and analysis of sequence data. *Bioinformatics*, 28, 1647–1649.
https://doi.org/10.1093/bioinformatics/bts199
Köhler, J., Jansen, M. Rodríguez, A., Kok, P.J.R., Toledo, L.F., Emmrich, M., Glaw, F., Haddad, C.F.B., Rödel, M. & Vences, M. (2017) The use of bioacoustics in anuran taxonomy: theory, terminology, methods and recommendations for best practice. *Zootaxa*, 4251 (1), 1–124.
https://doi.org/10.11646/zootaxa.4251.1.1
Kok, P.J.R. & Kalamandeen, M. (2008) Introduction to the taxonomy of the amphibians of Kaieteur National Park, Guyana. *Abc Taxa*, 5, 1–278.
Kumar, S., Stecher, G. & Tamura, K. (2015) MEGA7: Molecular Evolutionary Genetics Analysis Version 7.0 for Bigger Datasets. *Molecular Biology and Evolution*, 33 (7), 1870–1874.
https://doi.org/10.1093/molbev/msw054
Lanfear, R., Calcott, B., Ho, S.Y. & Guindon, S. (2012) PartitionFinder: combined selection of partitioning schemes and substitution models for phylogenetic analyses. *Molecular Biology and Evolution*, 29 (6), 1695–1701.
https://doi.org/10.1093/molbev/mss020
Lanfear, R., Frandsen, P.B., Wright, A.M., Senfeld, T. & Calcott, B. (2016) PartitionFinder 2: new methods for selecting partitioned models of evolution formolecular and morphological phylogenetic analyses. *Molecular Biology and Evolution*, 34 (3), 772–773.
https://doi.org/10.1093/molbev/msw260
Lourenço-de-Moraes, R., Ferreira, R.B., Fouquet, A. & Bastos, R.P. (2014) A new diminutive frog species of *Adelophryne* (Amphibia: Anura: Eleutherodactylidae) from the Atlantic Forest, southeastern Brazil. *Zootaxa*, 3846 (3), 348–360.
https://doi.org/10.11646/zootaxa.3846.3.2
Lynch, J.D. (1980) A new species of *Barycholos* from Estado Goiás, Brasil (Amphibia, Anura, Leptodactylidae) with remarks on related genera. *Bulletin du Museum National d'Histoire Naturelle, Paris, Section A, Zoologie, Biologie et Ecologie Animales,* 2, 289–302.
MacCulloch, R.D., Lathrop, A., Kok, P.J.R., Minter, L.R., Khan, S.Z. & Barrio-Amorós, C.L. (2008) A new species of Adelophryne (Anura: Eleutherodactylidae) from Guyana, with additional data on A. gutturosa. *Zootaxa*,1884, 36–50.
Miller, M.A., Pfeiffer, W. & Schwartz, T. (2010) Creating the CIPRES Science Gateway for inference of large phylogenetic trees. *Proceedings of the Gateway Computing Environments Workshop (GCE)*, New Orleans, LA, 2010, 1–8.
https://doi.org/10.1109/GCE.2010.5676129
Padial, J.M., Grant, T. & Frost, D.R. (2014) Molecular systematics of terraranas (Anura: Brachycephaloidea) with an assessment of the effects of alignment and optimality criteria. *Zootaxa*, 3825 (1), 1–132.
https://doi.org/10.11646/zootaxa.3825.1.1
Palumbi, S.R. (1996) Nucleic acids II: the polymerase chain reaction. *In*: Hillis, D.M., Moritz, C. & Mable, B.K. (Eds.), *Molecular Systematics*. Sinauer & Associates Inc., Sunderland, Massachusetts, pp. 205–247.
Peloso, P.L.V., Sturaro, M.J., Forlani, M.C., Gaucher, P., Motta, A.P. & Wheeler, W.C. (2014) Phylogeny, taxonomic revision,

and character evolution of the genera *Chiasmocleis* and *Syncope* (Anura, Microhylidae) in Amazonia, with descriptions of three new species. *Bulletin of the American Museum of Natural History*, 386 (1), 1–112.
https://doi.org/10.1206/834.1

Peloso, P.L.V., Orrico, V.G.D., Haddad, C.F.B., Lima-Filho, G.R. & Sturaro, M.J. (2016) A new species of clown tree frog, *Dendropsophus leucophyllatus* Species Group, from Amazonia (Anura, Hylidae). *South American Journal of Herpetology*, 11 (1), 66–80.
https://doi.org/10.2994/SAJH-D-16-00003.1

Real Academia Española (2014) *Diccionario de la lengua española. 23th Edition*. Available from: http://dle.rae.es (accessed 16 January 2017)

Simões, P.I. (2016) A new species of nurse-frog (Aromobatidae) from the Madeira River basin with a small geographic range. *Zootaxa*, 4083 (4), 501–525.
https://doi.org/10.11646/zootaxa.4083.4.3

Trancoso, R., Carneiro Filho, A., Tomasella, J., Schietti, J., Forsberg, B.R. & Miller, R.P. (2009) Deforestation and conservation in major watersheds of the Brazilian Amazon. *Environmental Conservation*, 36, 277–288.
https://doi.org/10.1017/S0376892909990373

Vaidya, G., Lohman, D.J. & Meier, R. (2011) SequenceMatrix: concatenation software for the fast assembly of multi?gene datasets with character set and codon information. *Cladistics*, 27, 171–180.
https://doi.org/10.1111/j.1096-0031.2010.00329.x

Vences, M., Thomas, M., Bonett, R.M. & Vieites, D.R. (2005) Deciphering amphibian diversity through DNA barcoding: chances and challenges. *Philosophical Transactions of the Royal Society B: Biological Sciences*, 360 (1462), 1859–1868.
https://doi.org/10.1098/rstb.2005.1717

Zwickl, D.J. (2006) *Genetic algorithm approaches for the phylogenetic analysis of large biological sequence datasets under the maximum likelihood criterion*. Ph.D. dissertation. The University of Texas at Austin, Austin, Texas.

APPENDIX 1. Origin and accession numbers of DNA sequences used in this study.

Taxon	Voucher	COI	16S	Locality	Coordinates	Reference
Adelophryne adiastola	Andes-A 2560 (AJC 2463)	JX298340	JX298299	Com. Puerto Vaupés, Colombia	1.198056° N, 70.2814° W	Fouquet *et al.* (2012)
Adelophryne baturitensis	MTR 14013	JX298321	JX298281	Ibiapaba, Ceará, Brazil	5.078753° S, 40.9334° W	Fouquet *et al.* (2012)
Adelophryne baturitensis	CFBHT 11100	JX298317	JX298277	Tiangua, Ceará, Brazil	3.709925° S, 40.9340° W	Fouquet *et al.* (2012)
Adelophryne gutturosa	PK 1168	JX298342	JX298302	Muri Muri creek, Kaieteur National Park, Guiana	5.277290° N, 59.4323° W	Fouquet *et al.* (2012)
Adelophryne maranguapensis	CFBHT 14119	JX298326	JX298286	Maranguape, Ceará, Brazil	3.890290° S, 38.7125° W	Fouquet *et al.* (2012)
Adelophryne pachydactyla	MTR 16244	JX298335	JX298294	Serra das Lontras, Arataca, Bahia, Brazil	15.18330° S, 39.3452° W	Fouquet *et al.* (2012)
Adelophryne pachydactyla	MTR 5988	JX298334	JX298293	Serra do Teimoso, Jussari, Bahia, Brazil	15.21091° S, 39.4809° W	Fouquet *et al.* (2012)
Adelophryne patamona	PK 1969	JX298337	JX298296	Mount Maringma, Guiana	5.219169° N, 60.5752° W	Fouquet *et al.* (2012)
Eleutherodactylus limbatus	CZACC 14.14087	KC776664	KC776683	Canon del Rio Maya, Maisi, Guantamo, Cuba	20.21359° N, 74.22787° W	Rodriguez *et al*. (2013)
Phyzelaphryne miriamae	MPEG 28548 (FPR 007)	MH483976	MH483972	Bragança, Rio Paraconi, Maués, Amazonas, Brazil	3.94711° S, 58.45627° W	This study
Phyzelaphryne miriamae	MPEG 41041 (PLVP 742)	MH483977	MH483973	Parque Nacional do Jaú, Amazonas, Brazil	2.29416° S, 62.45583° W	This study
Phyzelaphryne miriamae	MPEG 41044 (PLVP 754)	MH483978	MH483974	Parque Nacional do Jaú, Amazonas, Brazil	2.29416° S, 62.45583° W	This study
Phyzelaphryne miriamae	MPEG 41045 (PLVP 755)	MH483979	MH483975	Parque Nacional do Jaú, Amazonas, Brazil	2.29416° S, 62.45583° W	This study
Phyzelaphryne miriamae	SMS 629	JX298343	JX298303	Com. São Sebastião dos Bargas, Amazonas, Brazil	3.78943° S, 59.03405° W	Fouquet *et al.* (2012)
Phyzelaphryne miriamae	MTR 19141	JX298307	JX298347	Moio Bamba, right bank, Rio Purus, Amazonas, Brazil	4.72009° S, 62.13304° W	Fouquet *et al.* (2012)
Phyzelaphryne miriamae	MTR 19437	JX298346	JX298306	Moio Bamba, right bank, Rio Purus, Amazonas, Brazil	4.72009° S, 62.13304° W	Fouquet *et al.* (2012)
Phyzelaphryne miriamae	MTR 12700	JX298344	JX298304	Igarapé Açu, Rio Abacaxis, Amazonas, Brazil	4.34417° S, 58.63500° W	Fouquet *et al.* (2012)
Phyzelaphryne miriamae	MTR 12789	JX298345	JX298305	São Sebastião, Rio Abacaxis, Amazonas, Brazil	4.30889° S, 58.63639° W	Fouquet *et al.* (2012)
Phyzelaphryne miriamae	LSUMZ 16935	EU186689	—	Manaquiri, 40km south of Manaus, Amazonas, Brazil	3.61944° S, 60.44633° W	Hedges *et al.* (2008)
Phyzelaphryne nimio	MCP 13719	—	MG572225	ESEC Juami-Japurá, Canal da Inveja, Amazonas, Brazil	1.75834° S, 67.61532° W	This study

……*continued on the next page*

APPENDIX 1. (Continued)

Taxon	Voucher	COI	16S	Locality	Coordinates	Reference
Phyzelaphryne nimio	MCP 13710	—	MG572224	ESEC Juami-Japurá, Canal da Inveja, Amazonas, Brazil	1.75834° S, 67.61532° W	This study
Phyzelaphryne nimio	MCP 13711	—	MG572226	ESEC Juami-Japurá, Igarapé da Fartura, Amazonas, Brazil	1.96063° S, 67.93694° W	This study
Phyzelaphryne nimio	MCP 13687	—	MG572227	ESEC Juami-Japurá, Igarapé da Fartura, Amazonas, Brazil	1.96063° S, 67.93694° W	This study
Phyzelaphryne sp. (C1)	MTR 19206	JX298349	JX298309	Terra Vermelha, left bank, River Purus, Amazonas, Brazil	4.70215° S, 62.30907° W	Fouquet *et al.* (2012)
Phyzelaphryne sp. (C1)	FS 054	JX298348	JX298308	RDS do Uacari, left bank, River Juruá, Amazonas, Brazil	5.76257° S, 67.89884° W	Fouquet *et al.* (2012)
Phyzelaphryne sp. (C2)	Andes-A (JMP 2283)	JX298350	JX298310	Takana al Norte de la carretera Leticia, Senda Zafire, Colombia		Fouquet *et al.* (2012)
Phyzelaphryne sp. (C2)	Andes-A 832	JX298354	JX298314	Kilometer 13, Leticia, Colombia	4.111667° S, 69.9608° W	Fouquet *et al.* (2012)
Phyzelaphryne sp. (C2)	Andes-A 915	JX298353	JX298313	Kilometer 9–10, Leticia, Colombia	4.124167° S, 69.9414° W	Fouquet *et al.* (2012)
Phyzelaphryne sp. (C2)	Andes-A (JMP 2058)	JX298355	JX298315	Kilometer 13, Leticia, Colombia	4.111667° S, 69.9608° W	Fouquet *et al.* (2012)
Phyzelaphryne sp. (C2)	Andes-A 970	JX298351	JX298311	Varzea del arroyo Huallar, Leticia, Colombia	4.119490° S, 69.9510° W	Fouquet *et al.* (2012)
Phyzelaphryne sp. (C2)	Andes-A 971	JX298352	JX298312	Varzea del arroyo Huallar, Leticia, Colombia	4.119490° S, 69.9510° W	Fouquet *et al.* (2012)